Uehara, T., Bennett, B., Sakata, S.T., Satoh, Y., Bilter, G.K., Westwick, J.K., Brenner, D.A., 2005. JNK mediates hepatic ischemia reperfusion injury. Journal of Hepatology 42 (6), 850–859.

Wang, Y., Singh, R., Lefkowitch, J.H., Rigoli, R.M., Czaja, M.J., 2006. Tumor necrosis factor-induced toxic liver injury results from JNK2-dependent activation of caspase-8 and the mitochondrial death pathway. Journal of Biological Chemistry 281 (22), 15258–15267.

Yamamoto, K., Ichijo, H., Korsmeyer, S.J., 1999. Bcl-2 is phosphorylated and inactivated by ASK1/Jun N-terminal protein kinase pathway normally activated as G(2)/M. Molecular and Cellular Biology 19 (12), 8469–8478.

Yu, C., Minemoto, Y., Zhang, J., Liu, J., Tang, F., Bui, T.N., Xiang, J., Lin, A., 2004. JNK suppresses apoptosis via phosphorylation of the proapoptotic Bcl-2 family protein Bad. Molecular Cell 13 (3), 329–340.

Zhao, Y., Li, S., Childs, E.E., Kuharsky, D.K., Yin, X.M., 2001. Activation of pro-death Bcl-2 family proteins and mitochondria apoptosis pathway in tumor necrosis factor-alpha-induced liver injury. Journal of Biological Chemistry 276 (29), 27432–27440.

Please cite this article as: Takamura, M. et al. An inhibitor of c-*Jun* NH2-terminal kinase, SP600125, protects mice from D-galactosamine/lipopolysaccharide-induced hepatic failure... Life Sciences (2007), doi:10.1016/j.lfs.2006.12.034

Role of IP-10/CXCL10 in the progression of pancreatitis-like injury in mice after murine retroviral infection

Yusuke Kawauchi, Kenji Suzuki, Shiro Watanabe, Satoshi Yamagiwa, Hiroyuki Yoneyama, Gi Dong Han, Suresh S. Palaniyandi, Punniyakoti T. Veeraveedu, Kenichi Watanabe, Hiroshi Kawachi, Yoshiaki Okada, Fujio Shimizu, Hitoshi Asakura, Yutaka Aoyagi and Shosaku Narumi

Am J Physiol Gastrointest Liver Physiol 291:345-354, 2006. doi:10.1152/ajpgi.00002.2006

Am J Physiol Gastrointest Liver Physiol 291: G345–G354, 2006;
doi:10.1152/ajpgi.00002.2006.

Role of IP-10/CXCL10 in the progression of pancreatitis-like injury in mice after murine retroviral infection

Yusuke Kawauchi,[1] Kenji Suzuki,[1] Shiro Watanabe,[1] Satoshi Yamagiwa,[1] Hiroyuki Yoneyama,[2] Gi Dong Han,[3,6] Suresh S. Palaniyandi,[4] Punniyakoti T. Veeraveedu,[4] Kenichi Watanabe,[4] Hiroshi Kawachi,[3] Yoshiaki Okada,[5] Fujio Shimizu,[3] Hitoshi Asakura,[1] Yutaka Aoyagi,[1] and Shosaku Narumi[2]

Departments of [1]Gastroenterology and Hepatology and [3]Cell Biology, Institute of Nephrology, Niigata University Graduate School of Medical and Dental Sciences, Niigata; [5]Department of Bacterial and Blood Products, National Institute of Infectious Diseases, Tokyo; [2]Department of Molecular Preventive Medicine, University of Tokyo Graduate School of Medicine, Tokyo; [4]Department of Clinical Pharmacology, Niigata University of Pharmacy and Applied Life Sciences, Niigata, Japan; and [6]Department of Food Science and Technology, Yeungnam University, Gyeongsan, Republic of Korea

Submitted 4 January 2006; accepted in final form 1 April 2006

Kawauchi, Yusuke, Kenji Suzuki, Shiro Watanabe, Satoshi Yamagiwa, Hiroyuki Yoneyama, Gi Dong Han, Suresh S. Palaniyandi, Punniyakoti T. Veeraveedu, Kenichi Watanabe, Hiroshi Kawachi, Yoshiaki Okada, Fujio Shimizu, Hitoshi Asakura, Yutaka Aoyagi, and Shosaku Narumi. Role of IP-10/CXCL10 in the progression of pancreatitis-like injury in mice after murine retroviral infection. *Am J Physiol Gastrointest Liver Physiol* 291: G345–G354, 2006; doi:10.1152/ajpgi.00002.2006.—Exocrinopathy and pancreatitis-like injury were developed in C57BL/6 (B6) mice infected with LP-BM5 murine leukemia virus, which is known to induce murine acquired immunodeficiency syndrome (MAIDS). The role of chemokines, especially CXCL10/interferon (IFN)-γ-inducible protein 10 (IP-10), a chemokine to attract $CXCR3^+$ T helper 1-type $CD4^+$ T cells, has not been investigated thoroughly in the pathogenesis of pancreatitis. B6 mice were inoculated intraperitoneally with LP-BM5 and then injected every week with either an antibody against IP-10 or a control antibody. Eight weeks after infection, we analyzed the effect of IP-10 neutralization. Anti-IP-10 antibody treatment did not change the generalized lymphadenopathy and hepatosplenomegaly of mice with MAIDS. The treatment significantly reduced the number of IP-10- and CXCR3-positive cells in the mesenteric lymph nodes (mLNs) but not the phenotypes and gross numbers of cells. In contrast, IP-10 neutralization reduced the number of mononuclear cells infiltrating into the pancreas. Anti-IP-10 antibody treatment did not change the numbers of $IFN\text{-}\gamma^+$ and $IL10^+$ cells in the mLN but significantly reduced their numbers, especially $IFN\text{-}\gamma^+$ and $IL\text{-}10^+$ $CD4^+$ T cells and $IFN\text{-}\gamma^+$ $Mac\text{-}1^+$ cells, in the pancreas. IP-10 neutralization ameliorated the pancreatic lesions of mice with MAIDS probably by blocking the cellular infiltration of $CD4^+$ T cells and $IFN\text{-}\gamma^+$ $Mac\text{-}1^+$ cells into the pancreas at least at 8 wk after infection, suggesting that IP-10 and these cells might play a key role in the development of chronic autoimmune pancreatitis.

autoimmune pancreatitis; Sjögren's syndrome; murine acquired immodeficiency syndrome; chemokines; interferon-γ-inducible protein 10

CHEMOKINES, which are chemotactic cytokines, control the essential process of the attraction of leukocytes to the tissues in inflammation (1, 18). The chemokine family comprises two major subfamilies, termed CXC and CC according to the arrangement of the first two conserved cysteines, which are separated by one amino acid and are adjacent, respectively (1, 18). Interferon (IFN)-γ-inducible protein of 10 kDa (IP-10/CXCL10) is a member of the CXC chemokine family and a potent chemoattractant for activated T lymphocytes, natural killer cells, and monocytes (6, 17). It is also considered as a regulator of T helper (Th)1 inflammatory responses (26). The expression of IP-10 was elevated in several diseases such as ulcerative colitis (34), hepatitis (21), multiple sclerosis (31), and Sjögren's syndrome (SjS) (22), suggesting the involvement of IP-10 in the development of these diseases. It has been recently reported that IP-10 is expressed by β-cells of the islets of Langerhans, resulting in the preferential accumulation of $CXCR3^+$ T cells into the pancreas in a virus-induced Type I diabetic mouse model (7). Information about the role of chemokines in pancreatic diseases, however, is limited and needs further investigation (2, 28). In the pathogenesis of chronic pancreatitis, especially with autoimmune etiology, the role of chemokines such as IP-10 has not been investigated thoroughly.

The LP-BM5 murine leukemia virus (MuLV) is a retrovirus that is known to induce profound immunodeficiency with splenomegaly and generalized lymphadenopathy in susceptible strains of mice, such as C57BL/6 (B6) mice, and occasionally brings about lymphoid malignancy (10, 14, 19). In the early phase of infection, hypergammaglobulinemia and polyclonal B and T cell activation are induced and autoantibodies such as anti-nuclear and anti-double-stranded DNA antibodies are detected in mice infected with the virus (10, 14, 19). In the late phase of infection, virus-infected B6 mice show symptoms similar to those of human acquired immunodeficiency syndrome (AIDS); therefore, they have been studied as a murine model of AIDS, termed as murine AIDS (MAIDS) (10, 14, 19). We have reported previously that systemic exocrinopathy resembling SjS was induced in systemic exocrine glands such as salivary glands and lachrymal glands and in the pancreas of virus-infected mice; thus we proposed that mice with MAIDS could be an animal model for SjS as well as AIDS (32, 33). In mice with MAIDS, the pancreatic lesions are the exocrine system-oriented inflammation characterized by cellular infil-

Address for reprint requests and other correspondence: K. Suzuki, Dept. of Gastroenterology and Hepatology, Niigata Univ. Graduate School of Medical and Dental Sciences, 1-757 Asahimachi-dori, Niigata 951-8510, Japan (e-mail: kjsuzuki@med.niigata-u.ac.jp).

The costs of publication of this article were defrayed in part by the payment of page charges. The article must therefore be hereby marked "*advertisement*" in accordance with 18 U.S.C. Section 1734 solely to indicate this fact.

tration around the interlobular pancreatic ducts and acinar cell destruction (32, 33, 35), but with no damage of the endocrine system, that is, the islets of Langerhans (35). The pancreas-infiltrating cells comprise both Th1- and Th2-type $CD4^+$ T cells, although with a predominance of Th2 cells over Th1 cells (35). Thus the pancreatic lesions of the mice have some similarities to autoimmune-related chronic pancreatitis, especially the lesions associated with SjS.

To clarify the role of IP-10 in the development of chronic pancreatitis with autoimmune etiology, especially associated with SjS, we investigated the effect of CXCL10 neutralization on pancreatic lesions of mice with MAIDS. Our results suggest that anti-IP-10 monoclonal antibody ameliorated the pancreatic lesions of mice with MAIDS.

MATERIALS AND METHODS

Animals. Four-week-old female B6 mice were purchased from Charles River Japan (Kanagawa, Japan) and maintained at the Animal Center of the Niigata University School of Medicine under specific-pathogen-free conditions. All animal experiments were performed according to the "Guide for Animal Experiments" of Niigata University School of Medicine.

Induction of MAIDS. LP-BM5 MuLV was prepared from the supernatant of cloned G6 cells infected with the retrovirus as reported previously (35). Four-week-old B6 female mice were injected intraperitoneally with 0.3 ml of LP-BM5 MuLV virus stock solution. At 8 wk after virus inoculation, mice with MAIDS were killed by cervical dislocation under ether anesthesia, and their pancreases were removed for further analysis. For blocking experiments, PBS containing 100 μg/100 μl anti-CXCL10 monoclonal antibodies (36) or anti-human parathyroid-related peptide monoclonal antibodies, which was the IgG_1 subclass-matched control monoclonal antibody, or PBS alone were administered intraperitoneally at the time of virus inoculation and once a week thereafter.

Monoclonal antibodies. For immunofluorescence (IF) and flow cytometric analyses, the following monoclonal antibodies were used: anti-CD4 (clone GK1.5, IgG_{2b}), anti-CD8 (clone 53-6.7, IgG_{2a}), anti-B220 (clone RA3-6B2, IgG_{2a}), anti-Mac-1 (clone M-70.15, IgG_{2b}), anti-mouse INF-γ (clone XMG1.2), and anti-mouse IL-10 (clone JES5-16E3). For immunostaining of IP-10 or CXCR3, goat polyclonal antibodies to IP-10 or CXCR3 (Santa Cruz Biotechnology; Santa Cruz, CA) were used.

Detection of LP-BM5 MuLV by PCR. The PCR method used for the detection of the virus was as reported previously (33).

Quantitative RT-PCR to detect cytokine mRNA. Total RNA was extracted from the mesenteric lymph node (mLN) and pancreas specimens with TRIzol (GIBCO-BRL) according to the standard protocol and reverse transcribed. Thereafter, cDNA was amplified using the ABI 7700 sequence detector system (Applied Biosystems; Foster City, CA) with a set of primers and probes corresponding to IFN-γ, IL-10, IP-10, CXCR3, and GAPDH as previously described (36).

Histopathological examination. Tissue samples were taken from the pancreas, fixed in 10% buffered formalin, and then embedded in paraffin wax blocks. Sections (4-μm thick) were made in the usual way and stained with hematoxylin and eosin. The stained sections were then examined by light microscopy.

The numbers of inflammatory cells in a high-power field (×400) were counted under a microscope, and the degree of pancreatitis was assessed from *0* to *4* as reported previously (11, 24).

IF staining procedure. Frozen sections of the pancreas were prepared in a cryostat and stained with several fluorescent dye-conjugated anti-mouse antibodies as described above. The sections were observed by fluorescence microscopy.

Double-IF staining procedure. For the simultaneous demonstration of cell surface antigens and cytokines, the IF staining method was as reported previously (35).

Statistical analysis. Data are expressed as means ± SD. Statistical analyses were performed using the unpaired Student's *t*-test or the nonparametric Mann-Whitney test. Differences were considered significant at $P < 0.05$.

RESULTS

IP-10 neutralization did not prevent infection by the MAIDS virus. All mice infected with LP-BM5 MuLV developed characteristic MAIDS symptoms such as generalized lymphadenopathy and hepatosplenomegaly ($n = 15$), and neutralization of IP-10 did not change the course of MAIDS ($n = 15$). Eight weeks after the virus inoculation, there were no differences in the weights of the liver, spleen, and mLNs between mice with MAIDS injected with anti-IP-10 monoclonal antibody and those injected with control antibody (Fig. 1*A*). A defective LP-BM5 virus genome was detected in mice of both groups by

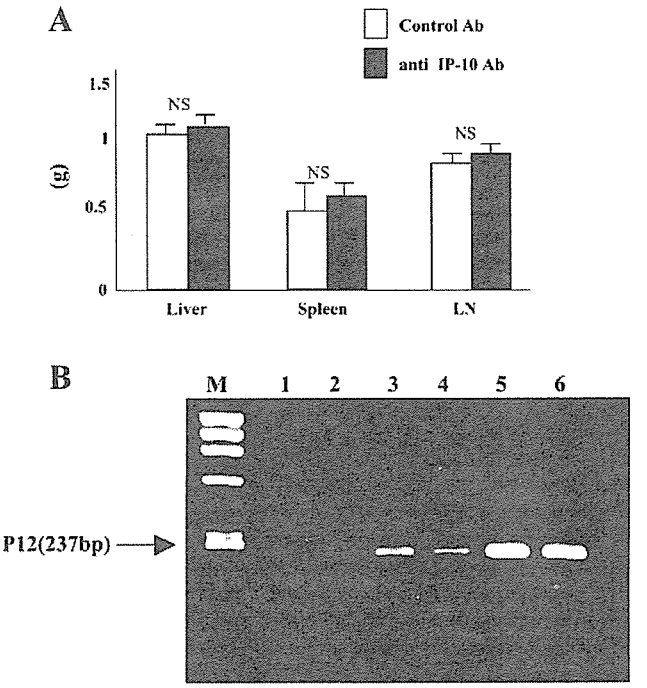

Fig. 1. Effect of neutralization of interferon (IFN)-γ-inducible protein of 10 kDa (IP-10/CXCL10) on the course of murine acquired immunodeficiency syndrome (MAIDS). *A*: effect of neutralization of IP-10 on organs of mice with MAIDS. The weights of the liver, spleen, and mesenteric lymph nodes (LNs) of mice with MAIDS injected with control antibody (Ab) were increased at 8 wk after infection. However, they were not changed after the injection of anti-IP-10 monoclonal (m)Ab. Data are means ± SD. NS, not significant. *B*: neutralization of IP-10 did not prevent infection by the MAIDS virus. LP-BM5 murine leukemia virus (MuLV) was detected in the mesenteric LNs and pancreas of mice with MAIDS at 8 wk after infection. Template DNAs were extracted from frozen sections of the pancreas and then analyzed by PCR with P12 primer. The bands were obtained by running the PCR products in agarose gel. M, molecular size marker; *lane 1*, the mesenteric LN of an uninfected C57BL/6 (B6) mouse (negative control); *lane 2*, the pancreas of an uninfected B6 mice (negative control); *lane 3*, the mesenteric LN of a mouse with MAIDS injected with control Ab; *lane 4*, the pancreas of a mouse with MAIDS injected with control Ab; *lane 5*, the mesenteric LN of a mouse with MAIDS injected with anti-IP-10 mAb; *lane 6*, the pancreas of a mouse with MAIDS injected with anti-IP-10 mAb.

PCR in the same frozen sections of the mLNs and pancreas of mice with MAIDS as those used for immunohistochemical staining (Fig. 1*B*). P12 of the virus genome was not detected in untreated normal B6 mice (Fig. 1*B*).

Effect of IP-10 neutralization on the expression of IP-10 and CXCR3 by lymphoid cells in mice with MAIDS. In the mLN and pancreas of mice with MAIDS injected with control antibody, the expression levels of mRNA for IP-10 and its receptor CXCR3 were significantly increased compared with untreated B6 mice (Fig. 2*A*). Neutralization of IP-10 down-regulated the expression of mRNA for IP-10 and CXCR3 in the mLNs and pancreas of mice with MAIDS (Fig. 2, *A* and *B*). Next, we analyzed their expressions in the pancreas and mLN by IF. In normal mice, IP-10 and CXCR3 were detected neither in the mLN nor in the pancreas, with the exception of a few $CXCR3^+$ cells scattered in the mLN (data not shown). The numbers of cells that expressed IP-10 and CXCR3 increased in the mLN and pancreas of mice with MAIDS injected with control antibody (Fig. 3*I*, *A* and *B*, and *II*, *A* and *B*). Double-color IF revealed that in the mLN, some $IP\text{-}10^+$ cells were $Mac\text{-}1^+$ cells and $CXCR3^+$ cells were mainly $CD4^+$ T cells (Fig. 3*I*, *C* and *D*). In the pancreas of mice with MAIDS, IP-10 and CXCR3 were mainly detected on some cells in an inflammatory cell focus around the pancreatic duct (Fig. 3*II*, *A* and *B*). Double-color IF showed that $IP\text{-}10^+$ cells were not positive for CD4, CD8, B220, and Mac-1 (Fig. 3*II*, *C*). It also revealed that $CXCR3^+$ cells were mainly $CD4^+$ T cells (Fig. 3*II*, *D*). Interestingly, IP-10 was also detected on some cells localized between the basal laminas that envelope each acinus of a minimal functional unit of the exocrine system of the pancreas (Fig. 3*II*, *A*, *inset*). Neutralization of IP-10 decreased the numbers of cells that expressed IP-10 or CXCR3 in the mLN (Fig. 3*I*, *E* and *F*) and pancreas (Fig. 3*II*, *E* and *F*) of mice with MAIDS.

Effect of IP-10 neutralization on mLN cells of mice with MAIDS. IF study of the mLN revealed that the numbers of $CD4^+$, $CD8^+$, $B220^+$, and $Mac\text{-}1^+$ cells were unchanged statistically by neutralization of IP-10 (Fig. 4*A*).

To reveal the systemic effect of IP-10 neutralization on cytokine production, we analyzed the number of IFN-γ- and IL-10-positive cells in the mLN of mice with MAIDS at 8 wk after infection by IF. We chose IFN-γ as a representative for a proinflammatory cytokine (or Th1 response) and IL-10 as a representative of an anti-inflammatory cytokine (or Th2). In mLNs of mice with MAIDS, there was no significant difference between the anti-IP-10 monoclonal antibody-treated group and the control antibody-treated group in IL-10- and IFN-γ-positive cells (Fig. 4*B*). IP-10 neutralization did not change the number of these cytokine-positive cells in the mLN of mice with MAIDS (Fig. 4*B*).

IP-10 neutralization ameliorated pancreatic lesions of mice with MAIDS. We have previously reported that periductal mononuclear cellular infiltration resembling autoimmune pancreatitis associated with SjS was detected in mice with MAIDS

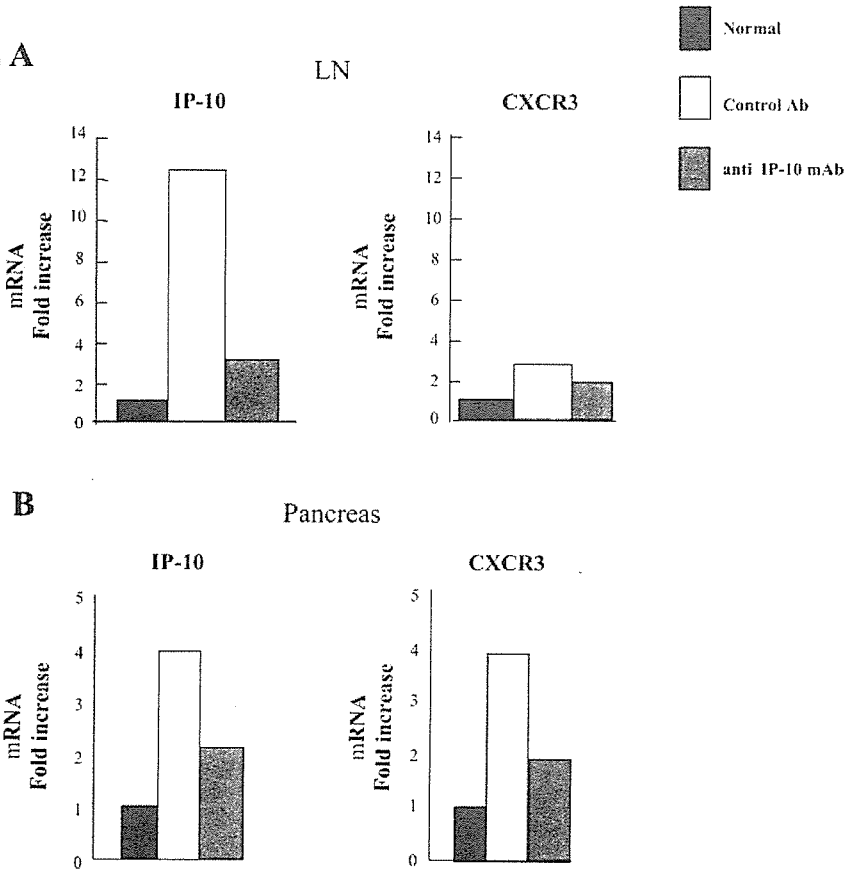

Fig. 2. Real-time quantitative PCR analysis of IP-10 and CXCR3 mRNA expression. The expressions of IP-10 and CXCR3 mRNA of the mesenteric LNs (*A*) and pancreas (*B*) were analyzed. Each amount was normalized to the level of each GAPDH. Final relative values are expressed relative to the calibrators (Ref. 36) as described above.

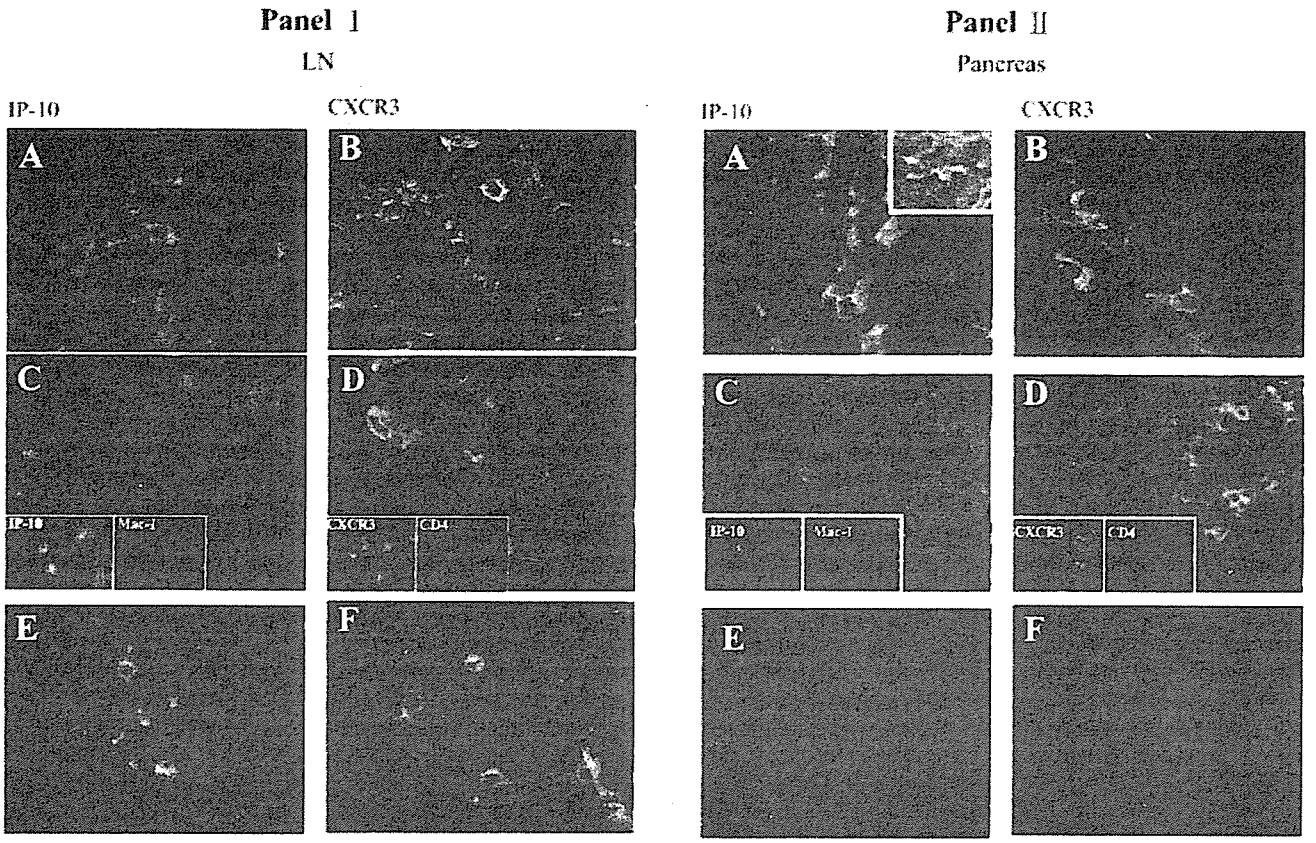

Fig. 3. *I*: effect of neutralization of IP-10/CXCL10 on the expressions of IP-10 and CXCR3 in the mesenteric LNs of mice with MAIDS. IP-10- and CXCR3-positive cells were detected in the mesenteric LNs of mice with MAIDS injected with control Ab (*A* and *B*). Their numbers decreased in the mesenteric LNs of mice with MAIDS injected with anti-IP-10 mAb (*E* and *F*). Some of the IP-10$^+$ cells (green) were Mac-1$^+$ cells (red), but were never positive for CD4, CD8, or B220 (*C*). Most of the CXCR3$^+$ cells (green) were positive for CD4 (red) (*D*). IP-10 was not detected, but CXCR3 was detected on a few cells in the mesenteric LN of an untreated B6 mouse (data not shown). *A*, *C*, and *E*, anti-IP-10 mAb-stained sections; *B*, *D*, and *F*, other sections stained with anti-CXCR3 Ab. *II*: effect of neutralization of IP-10 on the expressions of IP-10 and CXCR3 in the pancreas of mice with MAIDS. IP-10-and CXCR3-positive cells were detected in the pancreas of mice with MAIDS injected with control Ab (*A* and *B*). In the pancreas of mice with MAIDS, IP-10 and CXCR3 were mainly detected on some cells in a inflammatory cell focus around a pancreatic duct (*A* and *B*). Interestingly, IP-10 was also detected on cells localized between basal laminas that envelope each acinus of a minimal functional unit of the exocrine system of the pancreas (*A*, *inset*). IP-10$^+$ cells (green) were not positive for Mac-1$^+$ cells (red), CD4, CD8, or B220 (*C*). Most of the CXCR3$^+$ cells (green) were positive for CD4 (red) (*D*). IP-10 was not detected, but CXCR3 was detected on a few cells in the mesenteric LN of an untreated B6 mouse (data not shown). IP-10-and CXCR3-positive cells were not detected in the pancreas of mice with MAIDS injected with anti-IP-10 mAb (*E* and *F*). IP-10 and CXCR3 were not detected in the pancreas of an untreated B6 mouse (*A* and *B*). *A*, *C*, and *E*, sections stained with anti-IP-10 mAb; *B*, *D*, and *F*, sections stained with anti-CXCR3 Ab.

and the numbers of infiltrating cells and the grades of the lesions reached a peak at 8 wk after infection. To evaluate the effect of IP-10 neutralization, we, therefore, analyzed the pancreatic lesions of mice with MAIDS at 8 wk after infection. In mice with MAIDS injected with control antibody, inflammatory cells were detected around the pancreatic ducts, from where they progressively expanded, pressing the acinar architecture outward (Fig. 5*A*). At the interface lesions between the infiltrating cells and pancreatic parenchyma, destructed acinar cells were detected, but the degree of acinar cell destruction by infiltrating cells was rather mild (Fig. 5*C*). Peri-islet cellular infiltration was also observed (Fig. 5, *A* and *C*). Anti-IP-10 monoclonal antibody treatment clearly ameliorated the pathological lesions of the pancreas of mice with MAIDS (Fig. 5, *B* and *D*); the size of periductal cellular infiltration became smaller and the numbers of destructed acinar cells were also decreased (Fig. 5, *B* and *D*). Both the numbers of pancreas-infiltrating cells and the histological grading scores of the pancreatitis were significantly reduced by IP-10 neutralization (Fig. 5, *E* and *F*).

IP-10 neutralization ameliorated pancreatic lesions through decreased migration of CD4$^+$T, Mac-1$^+$, and B220$^+$ cells in mice with MAIDS. Eight weeks after infection, pancreas-infiltrating cells were composed of CD4$^+$ and CD8$^+$ T cells, Mac-1$^+$ macrophages, and B220$^+$ B cells but not natural killer cells or granulocytes. The major populations of infiltrating cells were composed CD4$^+$ T cells, Mac-1$^+$ macrophages, and B220$^+$ cells (Fig. 6, *A*, *C*, *E*, and *G*). The IF study showed that IP-10 neutralization significantly decreased the numbers of CD4$^+$ T, Mac-1$^+$, and B220$^+$ cells in pancreatic lesions of mice with MAIDS (Fig. 6, *B*, *D*, *F*, and *G*).

IP-10 neutralization decreased the migration of IFN-γ- and IL-10-producing CD4$^+$T and Mac-1$^+$ cells in the pancreas of mice with MAIDS. To reveal the effect of IP-10 neutralization on the immune response in the pancreas of mice with MAIDS, we analyzed the cytokine expression of IFN-γ and IL-10. The

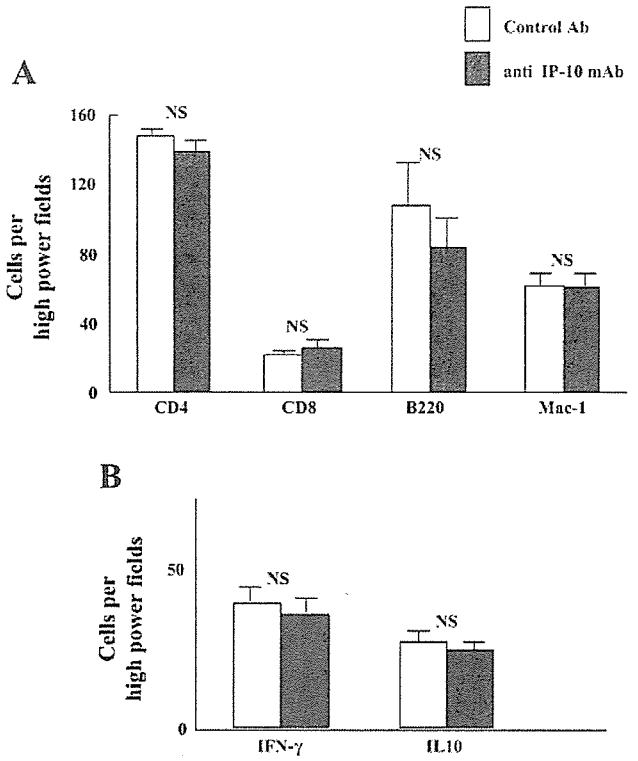

Fig. 4. Effect of neutralization of IP-10/CXCL10 on lymphocyte subpopulations in the LNs of mice with MAIDS. *A*: quantitative analysis of immune cells in the LNs by immunofluorescence (IF) for CD4, CD8, Mac-1, and B220. *B*: quantitative analysis of IFN-γ and IL-10 expression in the mesenteric LNs of mice with MAIDS at 8 wk after infection. Each focus of cellular infiltration was examined for the presence of CD4, CD8, B220, Mac-1, IFN-γ, and IL-10 cells. Final results are presented as the numbers of cells per high-powered microscope field. Representative findings (means ± SD; n = 10) from 3 independent experiments are shown.

levels of expression of the mRNAs of both cytokines in the pancreas were significantly increased after infection, and IP-10 neutralization decreased them (Fig. 7*A*). IF showed that IP-10 neutralization significantly decreased the numbers of IFN-γ- and IL-10-positive cells in the pancreas of mice with MAIDS (Fig. 7*B*).

Next, by the double-color IF method, we characterized the phenotypes of cells producing these cytokines. IFN-γ and IL-10 were mainly present on $CD4^+$ T cells (Fig. 8, *A* and *C*) and Mac-1^+ cells (Fig. 8, *E* and *G*) but not on $B220^+$ cells or $CD8^+$ T cells (data not shown). We did not detect the expression of IFN-γ or IL-10 in the pancreas of normal B6 mice (data not shown).

The numbers of IFN-γ- and IL-10-positive $CD4^+$ T cells were significantly reduced in mice with MAIDS by IP-10 neutralization (Figs. 7*C* and 8, *B* and D). Additionally, IP-10 neutralization significantly reduced the numbers of IFN-γ-positive Mac-1^+ cells in the pancreas of mice with MAIDS (Figs. 7*D* and 8*F*). The numbers of IL-10-positive Mac-1^+ cells became smaller by IP-10 neutralization, but there was no statistical significance between the mice with or without treatment (Figs. 7*D* and 8, *G* and *H*).

DISCUSSION

We have shown that systemic exocrinopathy including exocrine pancreatitis-like injury developed concordantly with the progression of MAIDS symptoms. Therefore, exocrine pancreatitis-like injury of mice with MAIDS might be a manifestation of several characteristic symptoms of MAIDS such as hepatomegaly, splenomegaly, systemic lymphadenopathy, and abnormal immunological reactions. In this study, we have shown that IP-10 neutralization ameliorated the pancreatic lesions of mice with MAIDS (Fig. 5) but prevented neither the infection nor the course of MAIDS (Fig. 1). These results suggest a different mechanism for the pathogenesis of systemic exocrinopathy including exocrine pancreatitis-like injury of MAIDS and the other MAIDS symptoms.

In the *Toxoplasma gondii* infection model, IP-10 neutralization inhibited the accumulation of effector T cells, resulting in a decreased ability to kill the parasite in target organs such as the liver, spleen, brain, and lung (12). IP-10 neutralization studies and a study on IP-$10^{-/-}$ mice also showed that the blockade of effector cell trafficking resulted in the breakdown of host defenses in neurotropic mouse hepatitis virus infection in the brain (5, 16). In the liver of patients with chronic active hepatitis C, we (21) have reported that IP-10 mRNA was expressed mainly in hepatocytes around intralobular focal and periportal piecemeal necrosis. These examples suggest that if the organ of the specific lesions induced by a particular infection was the same as the target organ of the infectious agent, IP-10 neutralization could ameliorate the organ lesions by inhibiting the trafficking of effector cells that eliminate the infectious agents from the target organ. In MAIDS, we reported previously that the virus was integrated in Ly-1 B cells but not in T cells (9) or on parenchymal cells of the pancreas (unpublished observations), although several reports have shown that B cells (13) and macrophages (4) as well as T cells (15) can serve as targets for infection of the virus. Therefore, pancreatic tissues are not the direct target cells of LP-BM5 infection, and the IP-10 neutralization-induced amelioration of pancreatic lesions of MAIDS cannot be explained by the decreased accumulation of effector cells that eliminate LP-BM5 from the pancreas.

We and others have reported that systemic exocrinopathy including pancreatitis-like injury is the characteristic organ lesions of mice with MAIDS (10, 14, 19, 32, 33, 35); however, the target antigen in exocrine glands, which regulates the target organ specificity, has been unknown. Without knowing the target antigen, delineating the process of inflammatory cell infiltration provides a basis for understanding the development of the pancreatic lesions of MAIDS. The blocking activity of the anti-IP-10 monoclonal antibody used in this study was confirmed in the chemotactic assay and in some other murine models depicting acute colitis (27) and encephalomyelitis (20). We confirmed that the anti-IP-10 monoclonal antibody had no cross-reactivity with other chemokines such as the monokine induced by IFN-γ, macrophage inflammatory protein-1α, or mature dendritic cells (36). In this study, therefore, we examined the expression of IP-10 and its receptor CXCR3 in the mLN and pancreas of mice with MAIDS. In the mLN and pancreas of MAIDS, IP-10 was mainly expressed on Mac-1^+ cells and CXCR3 was mainly detected on $CD4^+$ T cells. Anti-IP-10 treatment clearly reduced the number of these cells in both the mLN and pancreas. Our results suggest that cell trafficking into the pancreas of mice with MAIDS is carried out by the interaction between IP-10 and CXCR3 of $CD4^+$ cells. In the virus-induced Type I diabetes mouse model, it has been

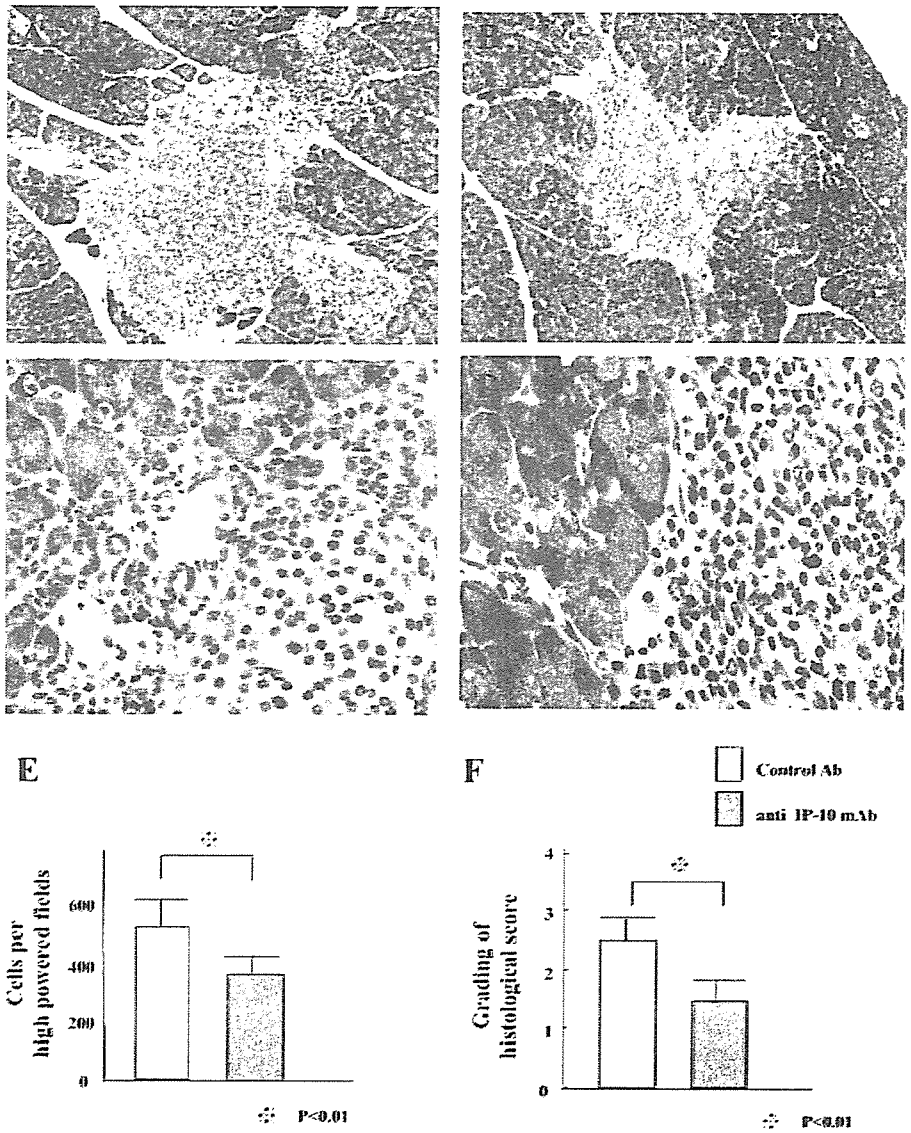

Fig. 5. Amelioration of pancreatic lesions of mice with MAIDS by neutralization of IP-10/CXCL10. *A* and *C*: pancreas from mice infected with LP-BM5 MuLV treated with control Ab at 8 wk after infection; *B* and *D*: pancreas from mice infected with LP-BM5 MuLV treated with anti-IP-10 mAb at 8 wk after infection. Sections were stained with hematoxylin and eosin. Original magnification: ×200 in *A* and *B* and ×400 in *C* and *D*. *E*: numbers of cells infiltrating the pancreas after infection. *F*: histological scores of acinar cell destruction of the pancreas at 8 wk after infection. Cells were counted under a microscope at high-power magnification for 3 different areas/mouse, and data of each time point were collected from 3 mice and compared with each other. *Data are significantly different between mice injected with anti-IP-10 mAb and those injected with control Ab as determined by Student's *t*-test ($P < 0.01$).

shown that β-cells of the islets of Langerhans produce chemokines including IP-10 with preferential attraction to T cells via CXCR3 (7). In our colitis model and those of others, IP-10 expression was confirmed in the colon epithelial cells, and IP-10 neutralization was shown to ameliorate the colitis with decreased $CXCR3^+$ cells in the colon (27, 29). In addition, Sugai et al. (22) reported that IP-10 is expressed on duct epithelial cells in salivary glands of patients with SjS. Contrary to these reports, we could not detect IP-10 expression on acinar cells or duct epithelial cells but found that IP-10 and CXCR3 were mainly expressed on cells in inflammatory foci around pancreatic ducts. Thus the lack of expression of IP-10 on target acinar cells and duct epithelial cells might be attributed to the mild pancreatitis-like injury of mice with MAIDS. Interestingly, IP-10 was also detected on cells localized between the basal laminas that envelope each acinus of a minimal functional unit of the exocrine system of the pancreas (Fig. 3*II*, *A*, *inset*). These cells disappeared together with the decreased numbers of pancreas-infiltrating cells after the neutralization of IP-10 (Fig. 3*II*, *A* and *C*). Therefore, we need to identify the nature of the $IP\text{-}10^+$ cells localized between basal laminas around each acinus, which are supposed to play a pivotal role in the recruitment of $CXCR3^+$ inflammatory cells into the pancreas of mice with MAIDS.

Recently, a Th1 and Th2 imbalance has been considered as one of the important mechanisms in the development of some autoimmune diseases (25). In our previous studies on the experimental models of encephalomyelitis (20), hepatitis (36), and Thy1.1 glomerulonephritis (8), we reported that anti-IP-10 monoclonal antibody treatment did not affect the cytokine environment of Th1/Th2 polarization. Considering these previous reports together with the observations of this study, it is conceivable that the IP-10 neutralization-induced amelioration of the pancreatic lesions of MAIDS did not result from the rectification of the cytokine environment of Th1/Th2 imbalance but rather from blockade of trafficking of inflammatory cells into the pancreas.

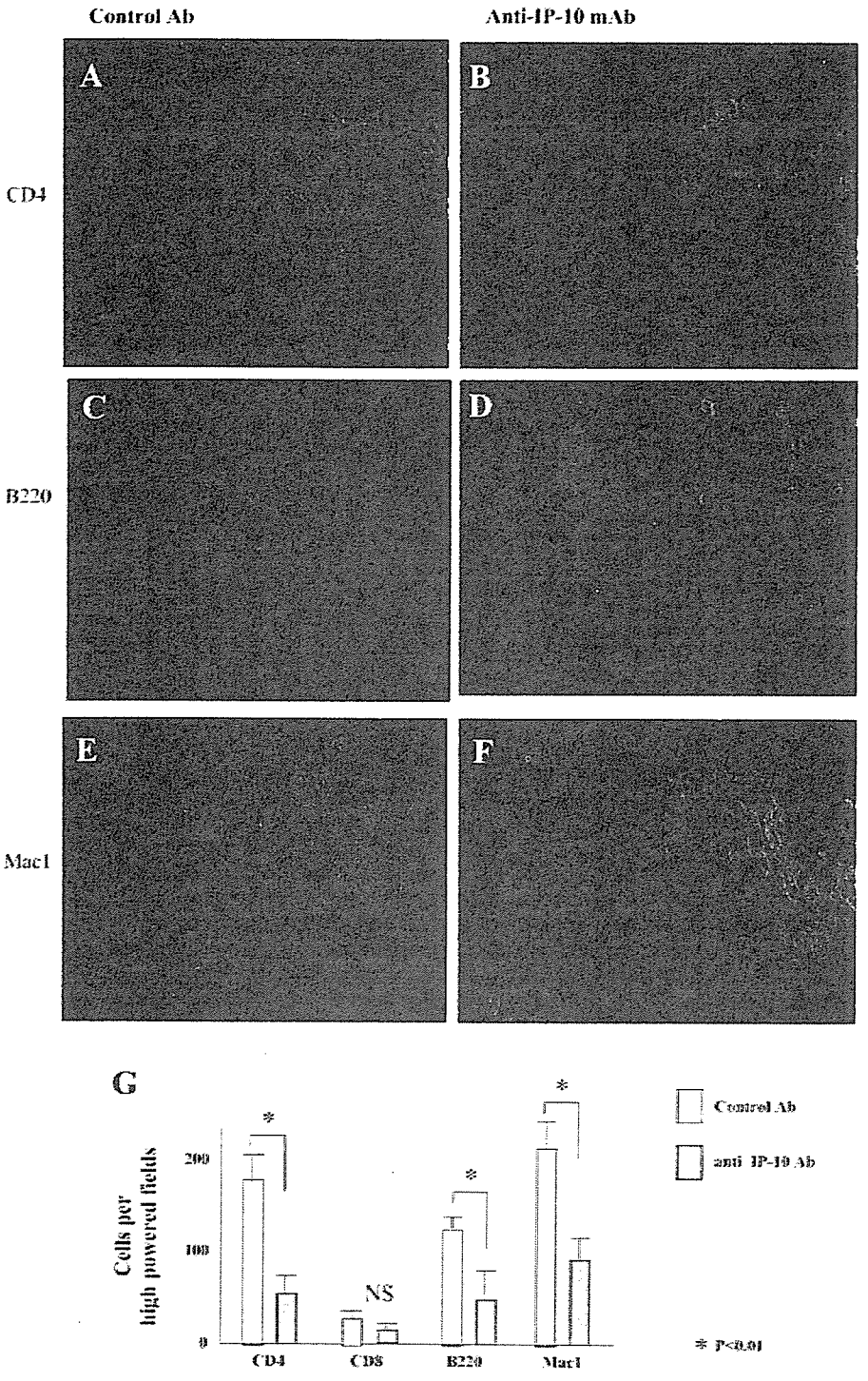

Fig. 6. Effect of neutralization of IP-10/CXCL10 on lymphocyte subpopulations in the pancreas of mice with MAIDS. IF analysis revealed the decreased numbers of CD4 (*A* and *B*), CD8 (data not shown), B220 (*C* and *D*), and Mac-1 (*E* and *F*) immune cells in the pancreas after blockade of IP-10. *G*: quantitative analysis of CD4, CD8, Mac-1, and B220 expression in the pancreas of mice with MAIDS at 8 wk after infection. Each focus of cellular infiltration was examined for the presence of CD4, CD8, B220, and Mac-1 cells. Final results are presented as the numbers of cells per high-powered microscope field. Representative findings (means ± SD; $n = 10$) from 3 independent experiments are shown. *Data are significantly different between mice injected with anti-IP-10 mAb and those injected with control Ab as determined by Student's *t*-test ($P < 0.01$).

In MAIDS, pancreas-infiltrating cells are mainly composed of $CD4^+$T cells, $B220^+$B cells, and Mac-1^+ macrophages (Fig. 6). Neutralization of IP-10 clearly and selectively decreased the numbers of these cells in the pancreas but not in the mLN of mice with MAIDS (Figs. 3–8). Flow cytometric analyses revealed the reciprocal quantitative change of cell phenotype between the mLN and pancreas. That is, IP-10 neutralization increased the numbers of $CD3^+$, $CD4^+$, and $\alpha\beta$T cells as well as Mac-1^+ cells in the mLN but decreased the numbers of those cells in the pancreas of mice with MAIDS (unpublished observations). These results suggest that IP-10 plays a pivotal role in the migration of inflammatory cells between the pancreas and mLN. IP-10-CXCR3 interactions, with Th1-dependent immunity, have been observed in several

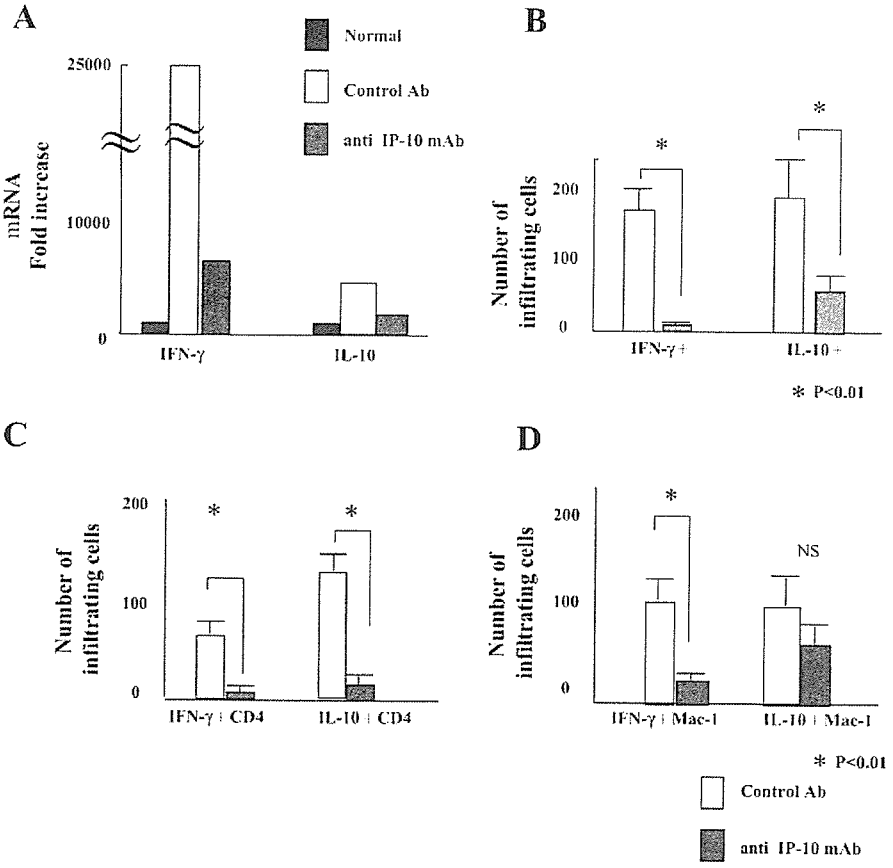

Fig. 7. Effects of blockade of IP-10/CXCL10 on cytokine production by inflammatory cells infiltrating the pancreas in mice with MAIDS. *A*: real-time quantitative PCR of IFN-γ and IL-10 mRNA expression in the pancreas of mice with MAIDS. Each amount was normalized to the level of GAPDH, and the final relative values are expressed relative to calibrators on *day 0*. *B*: numbers of pancreas-infiltrating cells that expressed IFN-γ and IL-10 at 8 wk after infection. Stained cryostat sections of 3 focuses of cellular infiltration of the individual pancreas were examined by counting the numbers of cells expressing IFN-γ and cells expressing IL-10. Three mice were analyzed for each time point. In control normal B6 mice, a negligible number of cells expressed IFN-γ or IL-10, so data are not shown. *C* and *D*: quantitative analysis of IFN-γ and IL-10 expression patterns of $CD4^+$ and Mac-1^+ cells that infiltrated the pancreas at 8 wk after infection. Stained cryostat sections of 3 focuses of cellular infiltration of the individual pancreas were examined by counting the numbers of $CD4^+$ cells expressing IFN-γ or IL-10 (*C*) and Mac-1^+ cells expressing IFN-γ or IL-10 (*D*). Three mice were analyzed for each time point. In control normal B6 mice, a negligible number of cells expressed IFN-γ or IL-10, so data are not shown. *Data are significantly different between mice injected with anti-IP-10 mAb and those injected with control Ab as determined by Student's *t*-test ($P < 0.01$).

inflammatory diseases, including multiple sclerosis (23, 30) and inflammatory bowel diseases (34). In animal models of these diseases, IP-10 neutralization or gene disruption of IP-10 clearly showed that amelioration of the diseases was achieved mainly by blocking $CXCR3^+$ cell trafficking into the IP-10-expressing target organs (5, 27, 29, 36). The ligands CXCL9, CXCL10, and CXCL11 bind to the CXCR3 receptor and share the ability to activate biochemical and functional events in target cells. All these ligands recruit $CXCR3^+$ cells; hence, neutralization of any of these ligands may not be sufficient to significantly abrogate the underlying biology of $CXCR3^+$ cells, but the use of CXCR3-deficient mice and IFN-γ neutralization will elucidate the role of these cells and cytokines in our model in future study. In this study, neutralization of IP-10 decreased not only the numbers of IFN-γ^+ $CD4^+$ T cells but also IL-10^+ $CD4^+$ T and IFN-γ^+ Mac-1^+ cells (Figs. 7 and 8). In an autoimmune diabetic mouse model injected with islet-specific Th1 $CD4^+$ T cells, insulitis was induced by the first accumulation of $CD4^+$ T cells followed by infiltration of Mac-1^+ cells (3). The inflammatory cells that infiltrated initially to the pancreas, therefore, might be the organ-specific autoreactive $CXCR3^+$ IFN-γ^+ $CD4^+$ T cells, and they then produce other cytokines and chemokines to attract the other IL-10^+ $CD4^+$ T cells and IFN-γ^+ Mac-1^+ cells into the pancreas of mice with MAIDS. In this study, we analyzed the effect of IP-10 neutralization only at one time point; however, the effects of the treatment on virus-induced inflammatory infiltrate and cytokine expression are most likely time dependent. Thus we need to analyze the kinetics of the responses in future study. IL-10^+ Mac-1^+ cells in the pancreatic lesions of mice with MAIDS were not significantly reduced by neutralization of IP-10 (Fig. 8), and the function of these cells in the formation of the lesions should be elucidated in future study. In conclusion, IP-10 neutralization could be a unique organ-specific therapeutic strategy for chronic pancreatitis, especially autoimmune pancreatitis associated with SjS.

ACKNOWLEDGMENTS

We thank Dr. Xiu-Hua Yang and Norio Honda for technical assistance and Dr. Minoru Nomoto and Dr. Terasu Honma for helpful discussions.

GRANTS

This work was supported by grants from the Ministry of Education and Science and Technology and the Ministry of Health, Welfare, and Labor of the Government of Japan.

REFERENCES

1. **Baggiolini M.** Chemokines and leukocyte traffic. *Nature* 392: 565–568, 1998.
2. **Bhatia M, Brady M, Shokuhi S, Christmas S, Neoptolemos JP, and Slavin J.** Inflammatory mediators in acute pancreatitis. *J Pathol* 190: 117–125, 2000.
3. **Bradley LM, Asensio VC, Schioetz LK, Harbertson J, Krahl T, Patstone G, Woolf N, Campbell IL, and Sarvetnick N.** Islet-specific Th1, but not Th2, cells secrete multiple chemokines and promote rapid induction of autoimmune diabetes. *J Immunol* 162: 2511–2520, 1999.
4. **Cheung SC, Chattopadhyay SK, Hartley JW, Morse 3rd HC, and Pitha PM.** Aberrant expression of cytokine genes in peritoneal macro-

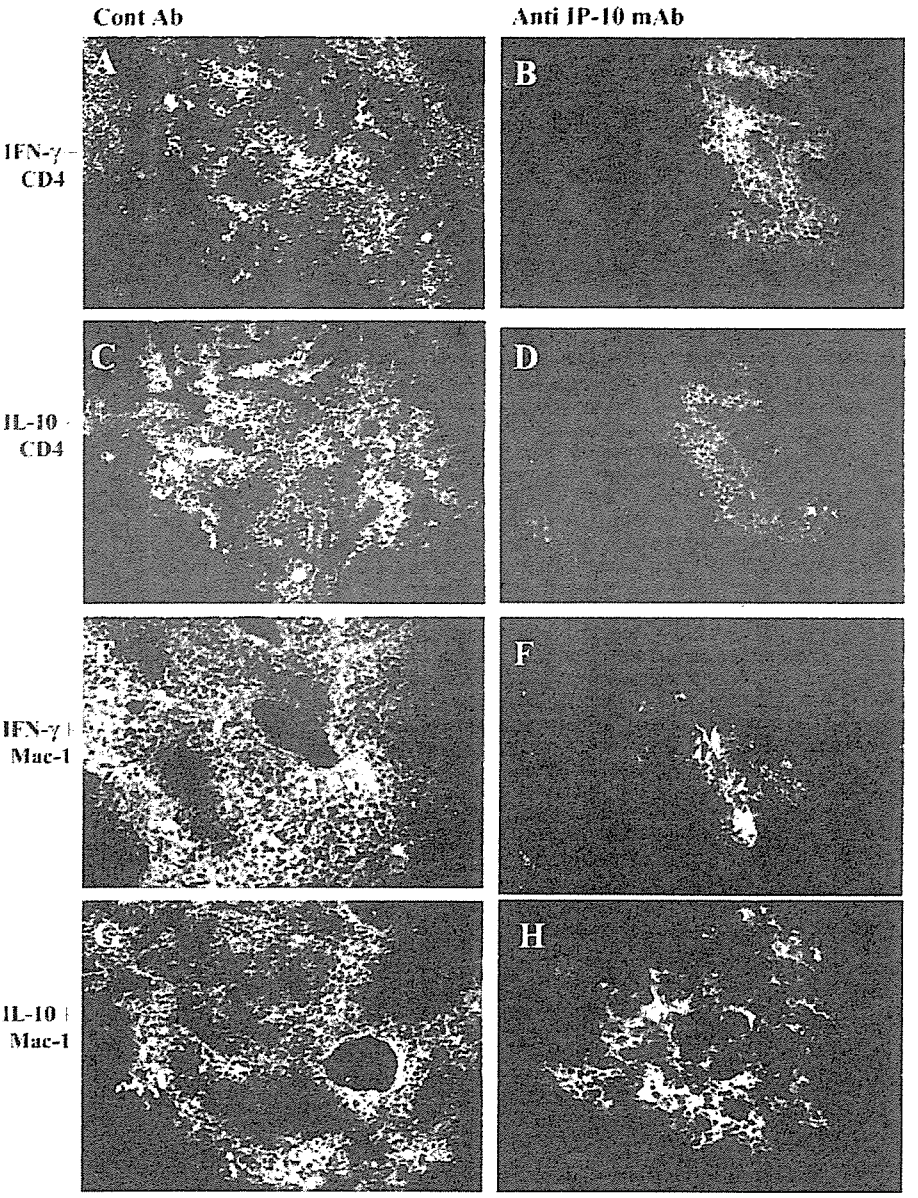

Fig. 8. Effects of blockade of IP-10/CXCL10 by a dual-labeling IF study of cytokine expression with cellular markers in the pancreas of mice with MAIDS. The numbers of cytokine-expressing cells were reduced by neutralization of CXCL10. Shown are sections of the pancreas of mice injected with control Ab (*A*, *C*, *E*, and *G*) or anti-IP-10 mAb (*B*, *D*, *F*, and *H*) at 8 wk after infection. *A–H*: double-color IF staining for CD4 and IFN-γ (*A* and *B*), CD4 and IL-10 (*C* and *D*), Mac-1 and IFN-γ (*E* and *F*), and Mac-1 and IL-10 (*G* and *H*) of the pancreas of mice with MAIDS at 8 wk after infection. *A–D*: CD4 (red); *E–H*: Mac-1 (red); *A*, *B*, *E*, and *F*: IFN-γ (green); *C*, *D*, *G*, and *H*: IL-10 (green).

phages from mice infected with LP-BM5 MuLV, a murine model of AIDS. *J Immunol* 146: 121–127, 1991.

5. **Dufour JH, Dziejman M, Liu MT, Leung JH, Lane TE, and Luster AD.** IFN-γ-inducible protein 10 (IP-10; CXCL10)-deficient mice reveal a role for IP-10 in effector T cell generation and trafficking. *J Immunol* 168: 3195–3204, 2002.
6. **Farber JM.** Mig and IP-10: CXC chemokines that target lymphocytes. *J Leukoc Biol* 61: 246–257, 1997.
7. **Frigerio S, Junt T, Lu B, Gerard C, Zumsteg U, Hollander GA, and Piali L.** β-Cells are responsible for CXCR3-mediated T-cell infiltration in insulitis. *Nat Med* 8: 1414–1420, 2002.
8. **Han GD, Koike H, Nakatsue T, Suzuki K, Yoneyama H, Narumi S, Kobayashi N, Mundel P, Shimizu F, and Kawachi H.** IFN-inducible protein-10 has a differential role in podocyte during Thy1.1 glomerulonephritis. *J Am Soc Nephrol* 14: 3111–3126, 2003.
9. **Hitoshi Y, Okada Y, Sonoda E, Tominaga A, Makino M, Suzuki K, Kinoshita J, Komuro K, Mizuochi T, and Takatsu K.** Delayed progression of a murine retrovirus-induced acquired immunodeficiency syndrome in X-linked immunodeficient mice. *J Exp Med* 177: 621–626, 1993.
10. **Jolicoeur P.** Murine acquired immunodeficiency syndrome (MAIDS): an animal model to study the AIDS pathogenesis. *FASEB J* 5: 2398–2405, 1991.
11. **Kannno H, Nose M, Itoh J, Taniguchi Y, and Kyogoku M.** Spontaneous development of pancreatitis in the MRL/Mp strain of mice in autoimmune mechanism. *Clin Exp Immunol* 89: 68–73, 1992.
12. **Khan IA, MacLean JA, Lee FS, Casciotti L, DeHaan E, Schwartzman JD, and Luster AD.** IP-10 is critical for effector T cell trafficking and host survival in *Toxoplasma gondii* infection. *Immunity* 12: 483–494, 2000.
13. **Kim WK, Tang Y, Kenny JJ, Longo DL, and Morse HC 3rd.** In murine AIDS, B cells are early targets of defective virus and are required for efficient infection and expression of defective virus in T cells and macrophages. *J Virol* 68: 5767–6769, 1994.
14. **Klinken SP, Fredrickson TN, and Hartley JW.** Evolution of B cell lineage lymphomas in mice with a retrovirus-induced immunodeficiency syndrome, MAIDS. *J Immunol* 140: 1123–1131, 1998.
15. **Kubo Y, Nakagawa Y, Kakimi K, Matsui H, Iwashiro M, Kuribayashi K, Masuda T, Hiai H, Hirama T, Yanagawa S, and Ishimoto A.**

Presence of transplantable T-lymphoid cells in C57BL/6 mice infected with murine AIDS virus. *J Virol* 66: 5691–5695, 1992.
16. **Liu MT, Chen BP, Oertel P, Buchmeier MJ, Armstrong D, Hamilton TA, and Lane TE.** The T cell chemoattractant IFN-inducible protein 10 is essential in host defense against viral-induced neurologic disease. *J Immunol* 165: 2327- 2330, 2000.
17. **Luster AD and Ravetch JV.** Biochemical characterization of a gamma interferon-inducible cytokine (IP-10). *J Exp Med* 166: 1084–1097, 1987.
18. **Luster AD.** Chemokines-chemotactic cytokines that mediate inflammation. *N Engl J Med* 338: 436–445, 1998.
19. **Mosier DE, Yetter RA, and Morse HC 3rd.** Retroviral induction of acute lymphoproliferative disease and profound immunosuppresion in adult C57BL/6 mice. *J Exp Med* 161: 766–784, 1985.
20. **Narumi S, Kaburaki T, Yoneyama H, Iwamura H, Kobayashi Y, and Matsushima K.** Neutralization of IFN-inducible protein10/CXCL10 exacerbates experimental autoimmune encephalomyelitis. *Eur J Immunol* 32: 1784–1791, 2002.
21. **Narumi S, Tominaga Y, and Tamaru M.** Expression of IFN-inducible protein 10 in chronic hepatitis. *J Immunol* 158: 5536–5544, 1998.
22. **Ogawa N, Ping L, Zhenjun L, Takada Y, and Sugai S.** Involvement of the interferon-γ-induced T cell-attracting chemokines, interferon-γ-inducible 10-kd protein (CXCL10) and monokine induced by interferon-γ (CXCL9), in the salivary gland lesions of patients with Sjögren's syndrome. *Arthritis Rheum* 46: 2730–2741, 2002.
23. **Qin S, Rottman JB, Myers P, Kassam N, Weinblatt M, Loetscher M, Koch AE, Moser B, and Mackay CR.** The chemokine receptors CXCR3 and CCR5 mark subsets of T cells associated with certain inflammatory reactions. *J Clin Invest* 101: 746–754, 1998.
24. **Qu WM, Miyazaki T, Terada M, Okada K, Mori S, Kanno H, and Nose M.** novel autoimmune pancreatitis model in MRL mice treated with polyinosinic:polycytidylic acid. *Clin Exp Immunol* 129: 27–34, 2002.
25. **Romagnani S.** The Th1/Th2 paradigm. *Immunol Today* 18: 263–266, 1997.
26. **Sallusto F, Lanzavecchia A, and Mackay CR.** Chemokines and chemokine receptors in T-cell priming and Th1/Th2-mediated responses. *Immunol Today* 19: 568–574, 1998.
27. **Sasaki S, Yoneyama H, Suzuki K, Suriki H, Aiba T, Watanabe S, Kawauchi Y, Kawachi H, Shimizu F, Matsushima K, Asakura H, and Narumi S.** Blockade of CXCL10 protects mice from acute colitis and enhances crypt cell survival. *Eur J Immunol* 32: 3197–3205, 2002.
28. **Saurer L, Reber P, Schaffner T, Buchler MW, Buri C, Kappeler A, Walz A, Friess H, and Mueller C.** Differential expression of chemokines in normal pancreas and in chronic pancreatitis. *Gastroenterology* 118: 356–367, 2000.
29. **Singh UP, Singh S, Taub DD, and Lillard JW Jr.** Inhibition of IFN-γ-inducible protein-10 abrogates colitis in IL-10−/− mice. *J Immunol* 171: 1401–1406, 2003.
30. **Sorensen TL, Tani M, Jensen J, Pierce V, Lucchinetti C, Folcik VA, Qin S, Rottman J, Sellebjerg F, Strieter RM, Frederiksen JL, and Ransohoff RM.** Expression of specific chemokines and chemokine receptors in the central nervous system of multiple sclerosis patients. *J Clin Invest* 103: 807–815, 1999.
31. **Sorensen TL, Trebst C, Kivisakk P, Klaege KL, Majmudar A, Ravid R, Lassmann H, Olsen DB, Strieter RM, Ransohoff RM, and Sellebjerg F.** Multiple sclerosis: a study of CXCL10 and CXCR3 co-localization in the inflamed central nervous system. *J Neuroimmunol* 127: 59–68, 2002.
32. **Suzuki K, Fujiwara M, and Mizuochi T.** Exocrinopathy resembling Sjoegren's syndrome induced by a murine retrovirus: implication for a new animal model. In: *Sjoegren's Syndrome: State of the Art*, edited by Homma M, Sugai S, and Tojo T. Amsterdam: Kugler, 1994, p.171–173.
33. **Suzuki K, Makino M, Okada Y, Kinoshita J, Yui R, Kanazawa H, Asakura H, Fujiwara M, Mizuochi T, and Komuro K.** Exocrinopathy resembling Sjoegren's syndrome induced by a murine retrovirus. *Lab Invest* 69: 430–435, 1993.
34. **Uguccioni M, Gionchetti P, Robbiani DF, Rizzello F, Peruzzo S, Campieri M, and Baggiolini M.** Increased expression of IP-10, IL-8, MCP-1, and MCP-3 in ulcerative colitis. *Am J Pathol* 155: 331–336, 1999.
35. **Watanabe S, Suzuki K, Kawauchi Y, Yamagiwa S, Yoneyama H, Kawachi H, Okada Y, Shimizu F, Asakura H, and Aoyagi Y.** Kinetic analysis of the development of pancreatic lesions in mice infected with a murine retrovirus. *Clin Immunol* 109: 212–223, 2003.
36. **Yoneyama H, Narumi S, Zhang Y, Murai M, Baggiolini M, Lanzavecchia A, Ichida T, Asakura H, and Matsushima K.** Pivotal role of dendritic cell-derived CXCL10 in the retention of T helper cell 1 lymphocytes in secondary lymph nodes. *J Exp Med* 195: 1257–1266, 2002.

IFN-Inducible Protein-10 Plays a Pivotal Role in Maintaining Slit-Diaphragm Function by Regulating Podocyte Cell-Cycle Balance

Gi Dong Han,*† Koichi Suzuki,* Hiroko Koike,* Kenji Suzuki,‡ Hiroyuki Yoneyama,§ Shosaku Narumi,§ Fujio Shimizu,* and Hiroshi Kawachi*

*Department of Cell Biology, Institute of Nephrology, ‡Department of Gastroenterology and Hepatology, Niigata University Graduate School of Medical and Dental Sciences, Niigata, Japan, †Department of Food Science and Technology, Yeungnam University, Gyeongsan, Republic of Korea; and §Department of Molecular Preventive Medicine, School of Medicine and Core Research and Evolutional Science and Technology, University of Tokyo, Tokyo, Japan

IFN-inducible protein-10 (IP-10/CXCL10) is a potent chemoattractant for activated T lymphocytes and was reported recently to have several additional biologic activities. In this study, the pathophysiologic role of IP-10 in the glomerular visceral epithelial cell (podocyte) was investigated. In cultured podocytes subjected to recombinant IP-10 treatment, the expression of slit-diaphragm (SD) components nephrin and podocin clearly was heightened. Rats that had puromycin aminonucleoside nephropathy and anti–nephrin antibody–induced nephropathy and were subjected to anti–IP-10 function-blocking antibody (anti–IP-10 mAb) treatment displayed a decrease in the protein level of SD components, as well as exacerbated proteinuria. For exploration of the mechanisms of this process, the interaction between IP-10 and the cell-cycle regulatory proteins was investigated. Cultured podocytes subjected to recombinant IP-10 treatment displayed an increase in the protein level of $p27^{Kip1}$, whereas the levels of cyclins E and A decreased. The expression of IP-10 and SD components was heightened by the treatment of siRNA of cyclin A, whereas these expressions were lowered by the treatment of siRNA of $p27^{Kip1}$. Proteinuric rats subjected to anti–IP-10 mAb treatment displayed a heightened expression of cyclin A from the early phase of the disease, which indicates that the anti–IP-10 mAb treatment exacerbates podocyte injury by disturbing the cell-cycle balance. These results raise the possibility that IP-10 could become a novel therapeutic target in nephrotic syndrome and several diseases with altered cell-cycle balance.

J Am Soc Nephrol 17: 442–453, 2006. doi: 10.1681/ASN.2004090755

IFN-inducible protein of 10 kD (IP-10/CXCL10), identified as a member of the CXC chemokine family (1), is reported to be expressed in a variety of cells (2–6) and to have several additional biologic activities, such as the modulation of the expression of adhesion molecules and the inhibition of cell proliferation and angiogenesis (7). We have demonstrated that IP-10 can inhibit directly the proliferation of epithelial cells in the murine acute colitis model (8). In our previous study, we reported that IP-10 and its receptor CXCR3 are expressed in glomerular visceral epithelial cells (podocytes) and that IP-10 in the podocyte maintains the differentiated structure and function of the podocyte in an autocrine manner (9).

Podocytes are highly specialized cells that are characterized by interdigitating foot processes and the slit diaphragm (SD) connecting the adjacent foot processes. Because the adjacent foot processes arise from the cell bodies of the neighboring cells, the SD is a highly differentiated intercellular junction. The SD is thought to function as a size-selective permeability barrier in the glomerular capillary wall, preventing the leak of plasma proteins into primary urine (10–12). During the past several years, some molecules have been reported to be associated with SD. Nephrin, identified as a gene product of *NPHS1* (the mutated gene of the Finnish type congenital nephrotic syndrome), is considered to be a component of the SD critical for maintaining the barrier function. Following nephrin (13,14), podocin (15,16) and CD2-associated protein (CD2AP) (17) are reported to be functional molecules of the SD. Some recent reports have shown that the expression of these SD components is affected in a variety of genetic and acquired diseases that manifest proteinuria (10,18). Investigations into the precise function of the SD and the regulatory mechanism that maintains the SD function surely will lead to the development of new, effective therapeutic strategies for treating nephrotic syndrome. Another important characteristic of the podocyte is that it is a terminally differentiated cell. Studies on the mechanism of the arrested podocyte cell cycle seem to be worth pursuing not only in the field of nephrology but also in that of cell biology.

The purpose of this study was to investigate whether IP-10 can be a therapeutic target in nephrotic syndrome. We analyzed

Received September 10, 2004. Accepted October 25, 2005.

Published online ahead of print. Publication date available at www.jasn.org.

Address correspondence to: Dr. Hiroshi Kawachi, Department of Cell Biology, Institute of Nephrology, Niigata University Graduate School of Medical and Dental Sciences, 1-757 Asahimachi-dori, Niigata, 951-8510, Japan. Phone: +81-25-227-2160; Fax: +81-25-227-0770; E-mail: kawachi@med.niigata-u.ac.jp

ISSN: 1046-6673/1702-0442

the kinetics of the expression of IP-10/CXCR3 and the role of IP-10 in two experimental models of nephrotic syndrome, puromycin aminonucleoside (PAN) nephropathy and anti–nephrin antibody (ANA)–induced nephropathy, both with SD dysfunction resulting in proteinuria. The second purpose of this study was to investigate the mechanism by which IP-10 maintains the differentiated podocyte phenotype. It was reported recently that the differentiated podocyte phenotype is maintained by the cell-cycle balance (19). The mammalian cell cycle is governed by the balance of positive and negative cell-cycle regulatory proteins, namely, the cyclins and cyclin-dependent kinase inhibitors (CKI), respectively. Cyclin E is responsible for the progression of the G1/S phase, whereas the S/G2/M phase is promoted by cyclins A and B. The phosphorylation of the retinoblastoma protein (pRb) contributes to the proliferation of cells in the late G1 phase (20,21). These cell-cycle activators are negatively regulated by CKI $p27^{Kip1}$ and $p57^{Kip2}$. Some studies have shown that the expression of CKI is lowered in podocyte diseases, such as focal segmental glomerulosclerosis, collapsing glomerulonephropathy, and nephrotic syndrome (22–24). In this study, we analyzed whether IP-10 contributes to the regulation of the expression of the cell-cycle regulatory proteins.

This study shows that IP-10 contributes to the regulation of the expression of SD components not only in the physiologic state but also in pathologic states. It is also demonstrated here that IP-10 regulates the cell-cycle balance of the podocyte. We propose here the heightening of the IP-10 function as one of the attractive therapeutic target candidates in nephrotic syndrome and a variety of diseases in which the negative regulation of the cell-cycle balance is altered.

Materials and Methods

Animals

All experiments were performed using specific pathogen-free female Wistar rats (6 wk old) that weighed 140 to 180 g (purchased from Charles River Japan, Atsugi, Japan). All animal experiments conformed to the National Institutes of Health Guide for the Care and Use of Laboratory Animals.

Culture of Podocyte

The conditionally immortalized mouse podocyte cell line was provided by Dr. Peter Mundel (Albert Einstein College of Medicine, Bronx, NY). Cultivation of differentiated immortalized mouse podocytes was conducted as reported previously (25). In brief, podocytes were maintained in RPMI 1640 medium (Nissui Pharmaceutical, Tokyo, Japan) supplemented with 10% FBS (Life Technologies Inc., Grand Island, NY), 100 U/ml penicillin (Banyu Pharmaceutical, Tokyo, Japan), and 0.1 mg/ml streptomycin (Meiji Seika Kaisha, Tokyo, Japan). To propagate podocytes, we cultivated cells at 33°C (permissive conditions), and the culture medium was supplemented with 10 U/ml mouse recombinant IFN-γ (rIFN-γ) (Pepro Tech EC, London, England) to enhance expression of a thermosensitive T-antigen. To induce differentiation, we maintained podocytes at 37°C without IFN-γ (nonpermissive conditions) for at least 1 wk before using in the experiment.

Immunohistochemical Studies

Tissue samples for the immunofluorescence (IF) studies were prepared as described previously (9). The frozen sections, 3 μm thick, were cut with a cryostat and stained with the following antibodies. The rabbit anti–cyclin E, rabbit anti–cyclin A, goat anti–IP-10, and goat anti-CXCR3 antibodies were commercially purchased from Santa Cruz Biotechnology, Inc. (Santa Cruz, CA). The rabbit anti-nephrin antibody (intracellular site) (26) and rabbit anti-podocin antibody (N-terminal site) (16) were prepared as reported previously. FITC-conjugated swine anti-rabbit IgG was used for anti–cyclin E, anti–cyclin A, anti-nephrin, and anti-podocin antibodies. These secondary antibodies were purchased from DAKO (Glostrup, Denmark). FITC-conjugated anti-goat IgG was used for anti–IP-10 and anti-CXCR3 antibodies. These secondary antibodies were purchased from Southern Biotechnology Associates (Birmingham, AL).

Western Blot Analysis

The rat glomeruli and conditionally immortalized podocyte were isolated with PBS that contained protease inhibitors and solubilized with SDS sample buffer (consisting of 5% SDS, 6% β-mercaptoethanol, 150 mmol/L NaCl, 10% glycerol, and 0.001% bromphenol blue in 250 mol/L Tris-HCl [pH 6.8]) with protease inhibitors. The insoluble material was removed by centrifugation at 15,000 × *g* for 10 min. The concentration was measured by the bicinchoninic acid method (Pierce Chemical, Rockford, IL), and the solubilized material was subjected to SDS-PAGE with 5, 10, or 12% acrylamide gel according to the method of Laemmli *et al.* (27) and transferred to a polyvinyl difluoride membrane (Bio-Rad, Hercules, CA) by electrophoretic transblotting for 30 min using Trans-Blot SD (Bio-Rad). After blocking with bovine skim milk, strips of the membranes were exposed to the primary antibodies as described above and additionally rabbit anti-$p27^{Kip1}$, rabbit anti-$p57^{Kip2}$, rabbit anti-pRb antibodies, and mouse anti-Rb mAb (Cell Signaling Technology Inc., Danvers, MA) and rabbit anti–β-actin antibody (Sigma, St. Louis, MO). After overnight incubation, the membranes were washed three times and then incubated with alkaline phosphatase–conjugated goat anti-rabbit IgG (Bio Source International, Tago Immunologicals, Camarillo, CA) or with alkaline phosphatase–conjugated anti-mouse IgG (Bio Source International, Tago Immunologicals). The reaction was developed with an alkaline phosphatase chromogen kit (5-bromo-4-chloro-3-indolil phosphate p-toluidine salt/nitro blue tetrazolium; Biomedica, Foster City, CA).

Reverse Transcription–PCR Analysis

Semiquantitative reverse transcription–PCR (RT-PCR) with glomerular total RNA and conditionally immortalized podocyte total RNA was performed basically according to the method described previously (9). The primers were designed according to the published sequences (Table 1). Negative controls without cDNA and positive controls of cDNA from Con-A–stimulated rat spleen cells were included.

Experimental Design

rIP-10 and Anti–IP-10 mAb Treatment of Cultured Podocytes. Podocytes cultured under nonpermissive conditions were treated as follows: Treatment 1, the cells were treated with medium that contained 10 ng/ml rIP-10 (RELIA tech GmbH, Braunschweig, Germany); treatment 2, the cells were treated with medium that contained 10 ng/ml rIP-10 after preincubation with 0.2 mg/ml anti–IP-10 mAb for 1 h; treatment 3, The cells were treated with medium without rIP-10 after preincubation with 0.2 mg/ml anti–IP-10 mAb; and treatment 4, the cells were treated with medium without both rIP-10 and anti–IP-10 mAb.

The cells were harvested after incubation with rIP-10 for 24 h. The optimal concentrations of rIP-10 and anti–IP-10 mAb were determined in preliminary experiments. mRNA expression of nephrin and podocin

Table 1. PCR primers used in this study[a]

Probe	Sense Primer Antisense Primer (5′ 3′)	Temp (°C)	Size (bp)	Reference or Accession No.
IP-10	TGT CGT TCT CTG CCT CGT GCT GAC CTT CTT TGG CTC ACC GCT	58	264	NM_139089
CXCR3	GCT GTG GCC GAT GTA CTG CTG G CCA GGT GAT AGG GGG TCC AGC	61	535	NM_053415
Nephrin	CTG ACT GGG CTG AAG CCT TCT AAG AGC ACA GGC AGC AGG GG	60	203	(26)
Nephrin[b]	AGC TGT GGA ATG TAA CCC GAG CTGG GGG GCA AAT CGG ACG ACA AG	61	404	AY183460
Podocin	CCT GTG AGT GGC TTC TTG TCC TC GGA GAC GCT TCA TAG TGG TTT GCA	59	378	(16)
Podocin[b]	CCT GCG AGT GGC TTC TTG TCC TC AGA GGC GCT TCA TGG TGG TTT GCA	59	378	AY050309
Podoplanin	GAG CGT TTG GTT CTG GGA CTC A AGG AAG AGG ATG GGG AAC AGG	58	549	NM_019358
Podocalyxin	AGC GAC AAA CCA GCC AAG CAA TG TGG TGA GGG CTT GCT GTG CTA T	58	351	AF109393
Cyclin A[b]	GGCCAGGAGATCACAGCAATC CAACCTCCACCAGCCAGTCC	62	472	Z26580
$p27^{Kip1b}$	CGT GAG AGT GTC TAA CGG GAG GCA GCA GGT CGC TTC CTC ATC	61	462	BC014296
GAPDH[c]	CTC TAC CCA CGG CAA GTT CAA GGA TGA CCT TGC CCA CAG C	60	515	(38)

[a]IP-10, IFN-inducible protein-10; GAPDH, glyceraldehyde-3-phosphate dehydrogenase.
[b]Primer for mouse.
[c]Primer for mouse and rat. Others, for rat.

in the harvested cells was analyzed by semiquantitative RT-PCR, and the protein levels of cell-cycle regulatory proteins, including cyclins E and A, CKI $p27^{Kip1}$ and $p57^{Kip2}$, retinoblastoma gene product (Rb), and phosphorylated Rb (pRb), were analyzed by Western blotting. Each set of experiments was repeated at least five times. The anti–IP-10 mAb was obtained by immunizing mice with rat CXCL10/Fc fusion protein as described previously (28).

Podocytes cultured under permissive conditions were also treated with rIP-10 or anti–IP-10 mAb for 24 or 48 h. After the treatment, the numbers of the cells were counted using a hemacytometer.

Small Interfering RNA. The small interfering RNA (siRNA) sequences that target cyclin A (National Center for Biotechnology Information accession no. Z26580; 25 nucleotides in length corresponding to positions 948 to 972 of open reading frame) and $p27^{Kip1}$ (National Center for Biotechnology Information accession no. BC014296; 21 nucleotides in length corresponding to positions 73 to 93 of open reading frame) were synthesized by iGENE Inc. (Tsukuba, Japan) and Qiagen Inc. (Dusseldorf, Germany), respectively. Control siRNA were purchased from Qiagen Inc. Before transfection, podocytes were cultured to a density of 70 to 80% at 37°C as described above and then were transfected with the siRNA using a Trans IT-TKO transfection reagent (Mirus, WI) or HiPerFect Transfection Reagent (Qiagen Inc.) protocols. Cells were harvested 48 h after siRNA treatment for RT-PCR and Western blots analyses. Podocytes cultured under permissive conditions were also treated with those siRNA and harvested in 48 h for counting the numbers of cells.

Studies in PAN and ANA Nephropathy. PAN nephropathy was induced in rats by the intravenous injection of 10 mg/100 g body wt PAN. ANA nephropathy was induced in rats by the intravenous injection of 8 mg/rat ANA (anti-nephrin antibody 5-1-6). Anti-nephrin mAb 5-1-6 was prepared as described previously (29). The rats were killed at 1 h after the induction of the disease, on days 1, 4, 9, and 28 of PAN nephropathy and at 1 h and days 1, 5, and 14 of ANA nephropathy (n = 5 per each time point). The right kidney was removed, weighed, cut into portions, and used for the assessment of IF. The left kidney and remaining portion of the right kidney were pooled in each group and used to prepare total glomerular RNA. Twenty-four-hour urine samples were collected just before the rats were killed. Urine protein concentrations were determined by colorimetric assay (Bio-Rad, Oakland, CA) using BSA as a standard. The kinetics of the expression of IP-10, CXCR3, nephrin, and podocin were analyzed by IF and semiquantitative RT-PCR. The staining of cyclins A and E was also analyzed.

***In Vivo* Anti–IP-10 mAb Function-Blocking Study.** Anti–IP-10 mAb (3 mg/100 g body wt) was injected intravenously into normal Wistar rats daily (n = 3). As a control, RVG1 was injected instead of anti–IP-10 mAb (n = 3). The kidneys of these rats were removed and used for the assessment of IF on day 5. The expression of $p27^{Kip1}$, cyclin A, and cyclin E was analyzed by IF.

Anti–IP-10 mAb (3 mg/100 g body wt) was injected intravenously into rats with PAN nephropathy and ANA nephropathy at 5 h after disease induction. The rats were treated daily with anti–IP-10 mAb until the day they were killed. As a control, RVG1 was injected instead of anti–IP-10 mAb. The kidneys of these rats were removed on days 9 and 21 for PAN nephropathy and on days 5 and 14 for ANA nephropathy (n = 5 per each time point of the model). The right kidney was weighed, cut into portions, and used for the assessment of IF. The glomeruli were isolated from the left kidneys, and the remaining portion of the right kidneys were pooled in each group and were placed into two tubes. One was used to prepare total glomerular RNA, and the other was used for glomerular lysate. Glomerular mRNA expression of podocyte-associated proteins (nephrin, podocin, podoplanin, and podocalyxin) and IP-10 was analyzed by RT-PCR. The protein level of nephrin and podocin was analyzed by Western blotting with glomerular lysate. Twenty-four-hour urine samples were collected on days 3, 5, 7, 9, 14, 21, and 28 in PAN nephropathy and on days 1, 3, 5, 7, 10, and 14 in ANA nephropathy. Urine protein concentrations were determined as described above. The expression of cyclin A on day 9 of PAN nephropathy and on day 5 of ANA nephropathy was analyzed by IF.

Statistical Analyses

All values are expressed as means ± SD. The statistical significance (defined as $P < 0.05$) was evaluated using the unpaired t test or Mann Whitney U test. Data were analyzed using the GraphPad InStat 3.05 (GraphPad Software Inc., San Diego, CA).

Results

rIP-10 Treatment Heightened Expression of SD Components in Cultured Podocytes

Heightened mRNA of the podocin and nephrin and heightened protein level of podocin were detected in the cultured podocytes treated with rIP-10 for 24 h. This effect was interfered with by the preincubation treatment with anti–IP-10 mAb. The expression of podocin and nephrin in cultured podocytes treated with anti–IP-10 mAb, without subsequent incuba-

tion of rIP-10, was lower compared with the control level (Figure 1).

Expression of IP-10 and CXCR3 Was Heightened in PAN and ANA Nephropathy, Whereas that of Nephrin and Podocin Was Lowered

The amount of 24-h proteinuria in PAN nephropathy was as follows: Day 1, 1.73 ± 0.7; day 9, 255.4 ± 43.2; and day 28, 20.1 ± 13.9. That in ANA nephropathy was as follows: Day 1, 48.8 ± 29.4; day 5, 188.9 ± 122.1; and day 14, 6.0 ± 3.5. mRNA expression of IP-10 was already heightened at 1 h in both PAN and ANA nephropathy. Although the heightened expression transiently declined on day 1, a clear increase in IP-10 was observed on day 9 of PAN and on day 5 of ANA nephropathy, when the amount of proteinuria peaked. In the ANA model, the mRNA expression of CXCR3 gradually increased from hour 1 to day 5, and the heightened expression continued to day 14. A CXCR3 expression pattern similar to that of the ANA model was seen in the PAN model, except for the lowered expression pattern on day 28.

By contrast, the mRNA expression of nephrin significantly decreased on day 1 and gradually recovered in both models. Lowered expression of podocin was also detected on day 1 in both models. The kinetics of the mRNA expression of these molecules is shown in Figure 2.

Figure 3 shows the kinetics of IF staining of IP-10, CXCR3, nephrin, and podocin in PAN and ANA nephropathy. The immunostaining intensity of IP-10 and CXCR3 was clearly heightened on day 5 in ANA and on day 9 in PAN nephropathy, when massive proteinuria was observed. The heightened staining was observed in the form of a quasi-linear pattern along the glomerular capillary wall. By contrast, the immunostaining intensity of nephrin and podocin was dramatically decreased at the peak of proteinuria in both models.

Blocking of IP-10 Exacerbates PAN and ANA Nephropathy

The anti–IP-10 mAb treatment resulted in significantly exacerbated proteinuria on days 7 and 9 in PAN and on days 3 and 5 in ANA nephropathy (Figure 4A). Anti–IP-10 mAb treatment enhanced the decrease in the mRNA expression of podocin and podoplanin in both models (Figure 4B). Anti–IP-10 mAb also lowered the mRNA expression of IP-10 in PAN nephropathy. Western blot quantification showed that anti–IP-10 treatment decreased the protein levels of podocin and nephrin in both PAN and ANA nephropathy (Figure 4C).

IF Staining of $p27^{Kip1}$ and Cyclins E and A Altered in PAN and ANA Nephropathy

The expression of $p27^{Kip1}$ was clearly detected in normal glomeruli, and it gradually decreased from day 1 to day 9 after induction of PAN. The gradually decreasing staining of $p27^{Kip1}$ was also observed in ANA nephropathy. The expression of cyclins E and A was weakly detected in normal glomeruli, and it gradually increased from day 1. The intensified staining of cyclins A and E became more remarkable on days 5 and 9 after the induction of PAN and ANA nephropathy, respectively, when massive proteinuria was observed (Figure 5).

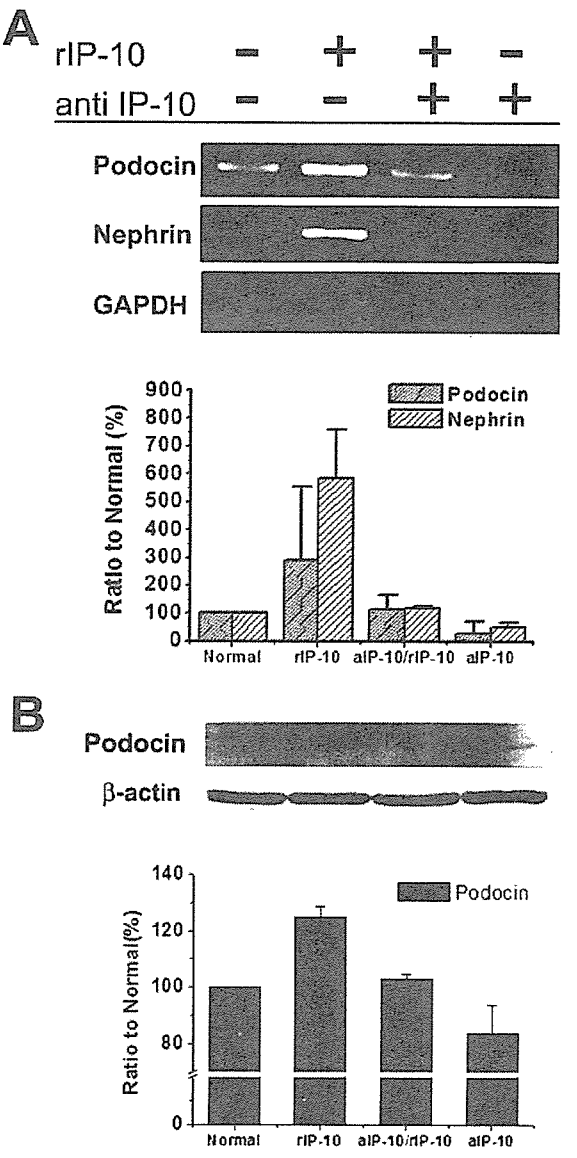

Figure 1. Reverse transcription–PCR (RT-PCR) and Western blot analyses of podocin and nephrin in murine cultured podocytes treated with recombinant IFN-inducible protein-10 (rIP-10). The cultured podocytes were incubated with rIP-10 for 24 h after preincubation with or without anti–IP-10 mAb. The mRNA expressions of podocin and nephrin (A) and protein level of podocin (B) were heightened as a result of the administration of rIP-10, and the effect was inhibited by preincubation with anti–IP-10 mAb. The expression of podocin and nephrin in cultured podocytes treated with anti–IP-10 mAb without subsequent incubation of rIP-10 was lower compared with the control level. The ratios of the densitometric signal of podocin and nephrin to that of the internal control (glyceraldehyde-3-phosphate dehydrogenase [GAPDH], β-actin) were analyzed. The data are shown as ratios (%) relative to the normal group and are expressed as mean ± SD of three independent experiments.

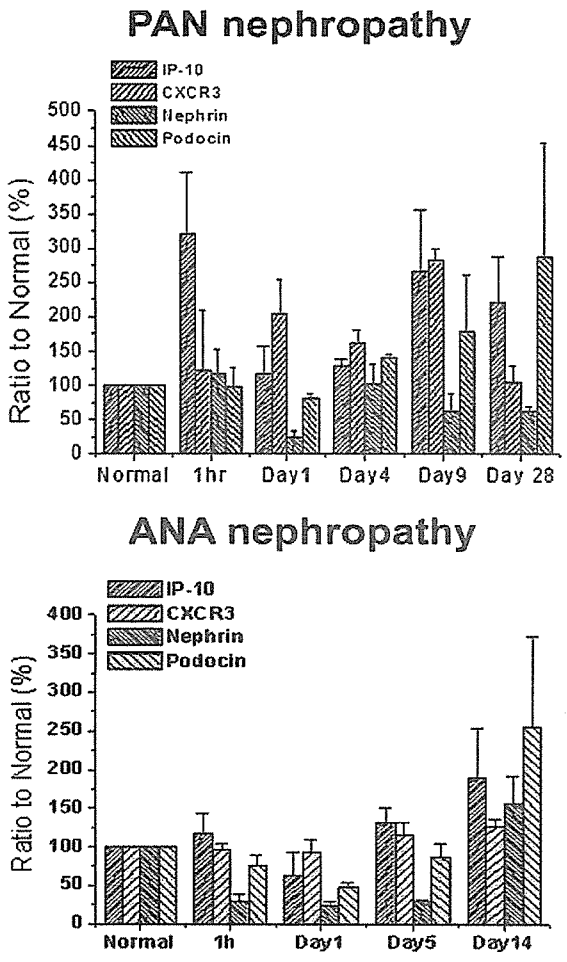

Figure 2. The kinetics of the mRNA expression of IP-10, CXCR3, and SD components in puromycin aminonucleoside (PAN) and anti–nephrin antibody (ANA) nephropathy. The mRNA expressions of IP-10, CXCR3, nephrin, and podocin were semiquantified by RT-PCR. The ratios of their densitometric signals to that of the internal control (GAPDH) were analyzed. The data are shown as ratios (%) relative to the RVG1-injected control group and are expressed as mean ± SD of three independent experiments. The mRNA expression of IP-10 and CXCR3 was heightened on days 9 and 5 after the induction of PAN and ANA nephropathy, respectively, when massive proteinuria was detected. By contrast, the mRNA expression of nephrin and podocin was significantly lower already on day 1 in both models and recovered or was heightened on days 28 and 14 of PAN and ANA nephropathy, respectively, at which time the proteinuria was normalized.

rIP-10 Treatment Altered Expression of Cell-Cycle Regulatory Proteins in Nonpermissive Conditioned Podocytes and Inhibited Proliferation of Permissive Conditioned Podocytes

Heightened expression of $p27^{Kip1}$ and lowered expression of cyclins A and E were detected in the cultured podocytes treated with rIP-10 for 24 h. Anti–IP-10 mAb pretreatment inhibited the effect of rIP-10. Anti–IP-10 mAb treatment without subsequent rIP-10 incubation resulted in a decrease in the $p27^{Kip1}$ level, and the treatment clearly increased the protein level of cyclin E, cyclin A, and pRb. No specific changes in the expression of $p57^{Kip2}$ and Rb were detected after these treatments (Figure 6A). The treatment with rIP-10 for 48 h inhibited the proliferation of permissive conditioned podocyte, whereas the treatment with anti–IP-10 for 24 and 48 h enhanced the proliferation (Figure 6B).

siRNA of Cyclin A and $p27^{Kip1}$ Affected Expression of IP-10 and SD Components

The treatment with siRNA for cyclin A and $p27^{Kip1}$ clearly silenced the expression of each target molecule in both mRNA and protein levels in nonpermissive conditioned podocyte. The treatment with siRNA for cyclin A enhanced the expressions in both mRNA (Figure 7A) and protein (Figure 7B) levels of IP-10 and SD components, whereas the siRNA treatment for $p27^{Kip1}$ lowered them. The treatment with siRNA for cyclin A for 48 h inhibited the proliferation of permissive conditioned podocyte, whereas the treatment with siRNA of $p27^{Kip1}$ for 48 h enhanced it (Figure 7C).

Daily Anti–IP-10 mAb Injections into Normal Rats Lowered Expression of $p27^{Kip1}$ and Enhanced Expression of Cyclins E and A

Daily anti–IP-10 mAb treatment for 5 d lowered the expression of $p27^{Kip1}$, whereas the anti–IP-10 mAb treatment enhanced the expression of cyclins E and A in the glomeruli (Figure 8).

Blocking of IP-10 Heightened Expression of Cyclin A in PAN and ANA Nephropathy

Daily injection with anti–IP-10 mAb promoted the increase of cyclin A expression on days 5 and 9 after the induction of ANA and PAN nephropathy, respectively, when massive proteinuria was observed (Figure 9).

Discussion

Podocytes, which are highly specialized, terminally differentiated cells, are characterized by the SD, a unique cell–cell junction structure. The SD plays a critical role in maintaining the barrier function of the glomerular capillary wall, preventing the leak of plasma proteins into urine. It is now accepted that SD dysfunction is involved in the development of proteinuria in a variety of diseases (11,30). IP-10, a CXC chemokine, is reported to have multiple functions, such as the regulation of the adhesion molecules and the inhibition of cell proliferation and angiogenesis. In the previous report, we showed that IP-10 contributes to the regulation of the expression of SD components. We also showed that anti–IP-10 function-blocking antibody treatment exacerbates mesangial alteration by disturbing the podocyte function (9). In this study, we first investigated whether the regulation of the IP-10 function can be a therapeutic target in podocyte injuries that manifest massive proteinuria.

We started this study to investigate whether rIP-10 treatment affects the expression of the differentiated podocyte molecules of the cultured podocytes, because in the previous report, we

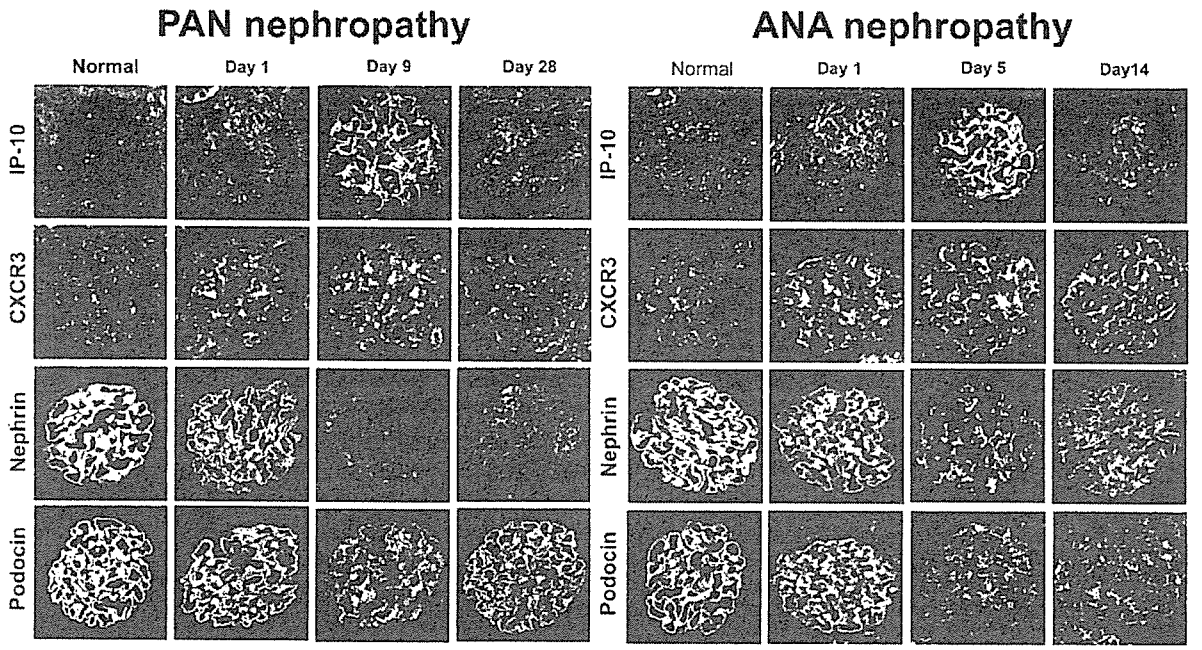

Figure 3. The kinetics of immunofluorescence (IF) staining of IP-10, CXCR3, nephrin, and podocin in PAN and ANA nephropathy. The immunostaining intensity of IP-10 and CXCR3 was clearly higher on day 9 of PAN and on day 5 in ANA nephropathy, when massive proteinuria was observed. The intensified staining was observed in the form of a linear pattern along the glomerular capillary wall. By contrast, the immunostaining intensity of nephrin and podocin was dramatically lower at the peak of proteinuria in both models. Magnification, ×400.

did not offer direct evidence for the capacity of IP-10 to enhance the expression of these molecules. As shown in Figure 1, IP-10 enhanced the mRNA expression of the SD components nephrin and podocin and also the protein expression of podocin, and this effect was inhibited by anti–IP-10 mAb. These *in vitro* findings and the *in vivo* findings in the previous report clearly show that IP-10 is involved in maintaining the differentiated podocyte phenotype in the physiologic state. Next, we analyzed the expression of IP-10 and its receptor CXCR3 in the podocyte in pathologic states. In this study, we adopted two rat models of podocyte injury, PAN nephropathy and ANA nephropathy. PAN nephropathy is widely used as a model of human minimal change-type nephropathy (31). ANA nephropathy is a model of proteinuria that is caused directly by nephrin dysfunction. In concordance with the previous report, the expression of nephrin and podocin clearly decreased in both models (16,26), when massive proteinuria was detected (Figures 2 and 3). By contrast, the expression of IP-10 and CXCR3 was markedly heightened at those time points (Figures 2 and 3). It is conceivable that the heightened expression of IP-10/CXCR3 is a protective response by which podocytes maintain their function, because the findings obtained in this and the previous studies suggest that IP-10 plays a role in maintaining the expression of SD components. To clarify this mechanism, we then analyzed the effect of anti–IP-10 function-blocking antibody administration on the severity of these podocyte injuries. We observed that anti–IP-10 function-blocking antibody treatment exacerbated proteinuria in both models by promoting the decrease in the expression of SD components (Figure 4), which suggests that IP-10 contributes to the expression of SD components not only in the physiologic state but also in pathologic states. Although the expression of IP-10 in human glomeruli is not precisely outlined yet in other reports, we have found that IP-10 is expressed in the form of an epithelial pattern along the glomerular capillary wall in humans as well as in rats (data not shown). All of these findings suggest that the heightening of the IP-10 function could be a therapeutic target in nephrotic syndrome.

The next important question that should be asked is how the podocyte maintains its differentiated phenotype. It was reported recently that the differentiated podocyte phenotype is maintained by the cell-cycle balance (19). In this study, we analyzed the immunohistochemical staining of the cell-cycle regulatory proteins of the podocyte in the normal rat and in experimental models of podocyte injury with massive proteinuria, PAN and ANA nephropathy. Although $p27^{Kip1}$ staining of the normal rat glomeruli was detected mainly in the mesangial area, the staining along the capillary wall was also observed (Figure 5). The decreased expression of $p27^{Kip1}$ in glomeruli was observed when massive proteinuria was detected. No Rb or pRb staining was detected in the glomeruli. By contrast, cyclins A and E were observed in the form of podocyte patterns along the glomerular capillary wall. Heightened expression of cyclins A and E was already detected on day 1 after disease induction in both models, when abnormal proteinuria had not occurred yet. In both models, the intensified staining of cyclins A and E became more remarkable when massive proteinuria was detected. In both models, the staining of cyclins A

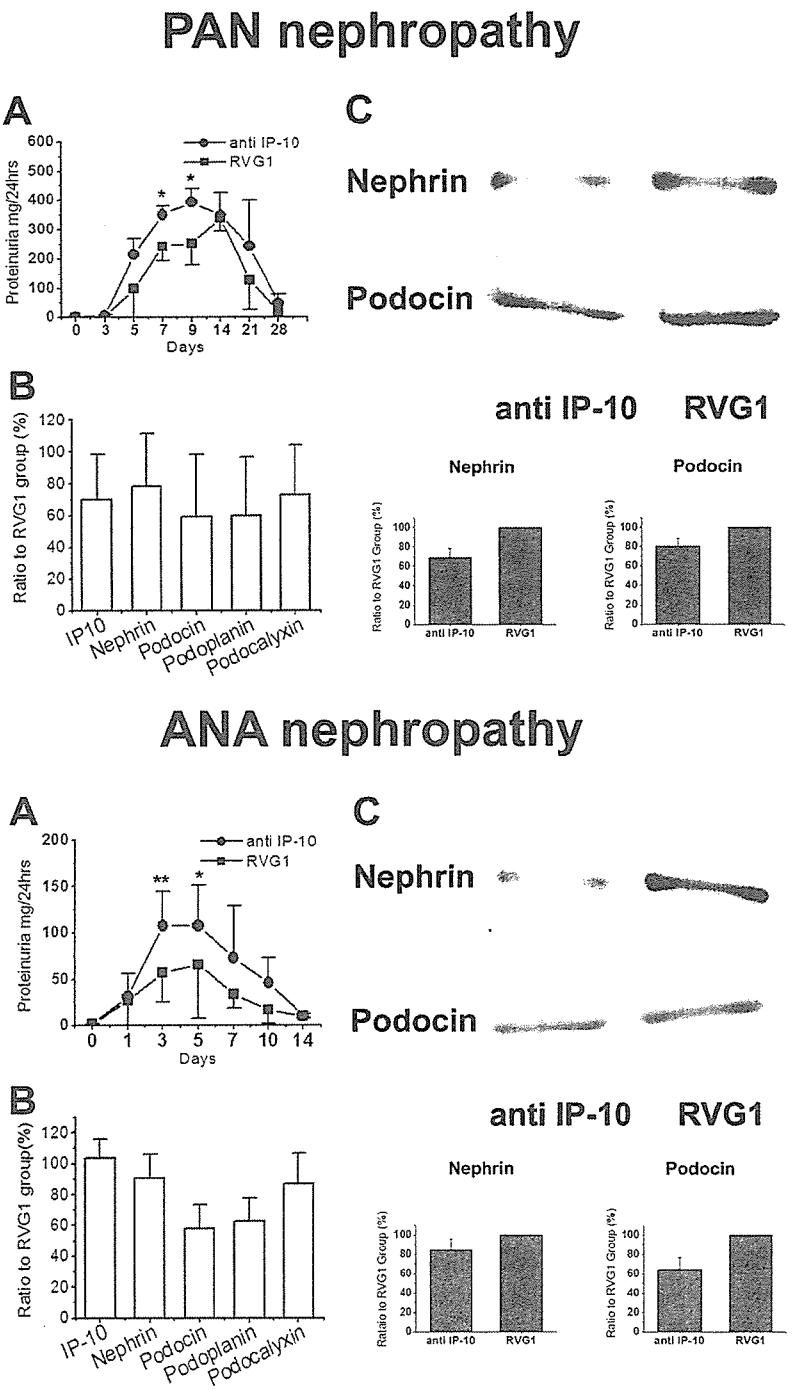

Figure 4. The effect of anti–IP-10 mAb treatment on PAN and ANA nephropathy. Effect of anti–IP-10 mAb (5 mg/100 g body wt) treatment on the kinetics of proteinuria (A), the mRNA expression of podocyte-associated proteins (B), and the protein level of nephrin and podocin (C) were analyzed. Daily injection with anti–IP-10 mAb exacerbated the proteinuria on days 7 and 9 and on days 3 and 5 after the induction of PAN and ANA nephropathy, respectively (A). mRNA (B) and Western blot (C) samples were prepared from the rats of days 9 and 5 after the induction of PAN and ANA nephropathy, respectively, when massive proteinuria was observed. The anti–IP-10 mAb treatment enhanced the decrease in the mRNA and protein levels of podocyte-associated molecules in both models (B and C). Equal amounts (250 μg) of solubilized glomerular lysate from the anti–IP-10 treatment group and the control group were loaded onto each lane. For ensuring equal loading, the translated membrane of each group was stained with Coomassie Brilliant Blue. Each Western blot was performed three times. Data are expressed as mean ± SD ($n = 5$; $^*P<0.05$, $^{**}P < 0.01$ *versus* the control group).

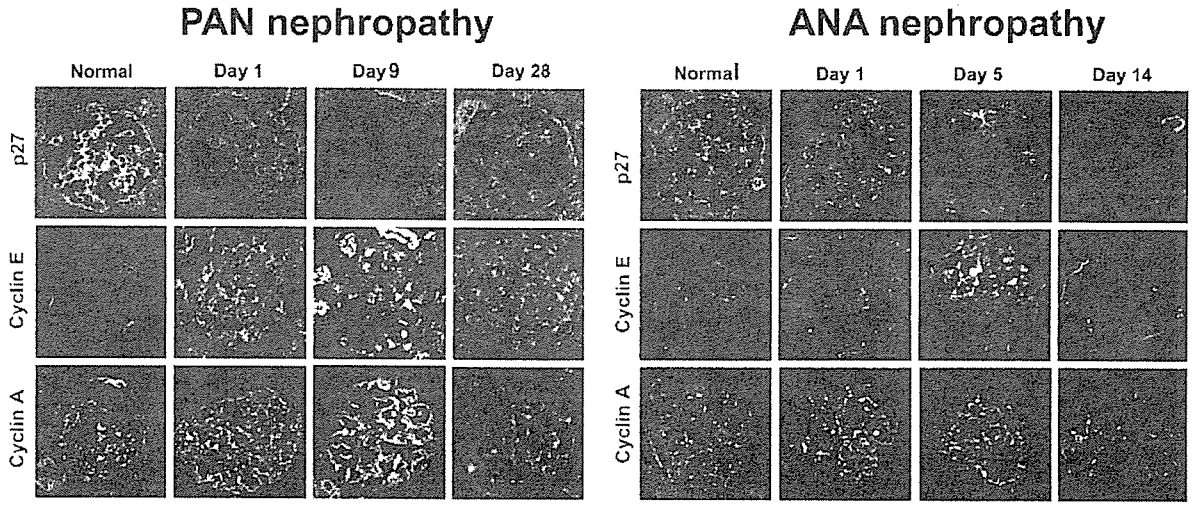

Figure 5. The kinetics of IF staining of $p27^{Kip1}$ and cyclins E and A in PAN and ANA nephropathy. The expression of $p27^{Kip1}$ was clearly detected in normal glomerular section and gradually decreased from day 1 to day 9 and day 5 after induction of PAN and ANA nephropathy, respectively. Heightened expression of cyclins E and A was already detected on day 1 after disease induction in both models. The intensified staining of cyclins E and A became more remarkable on days 9 and 5 after the induction of PAN and ANA nephropathy, respectively, when massive proteinuria was observed. Magnification, ×400.

and E returned to normal when proteinuria was normalized (Figure 5). These findings clearly show that the cell-cycle balance of the podocyte is altered in these proteinuric states caused by SD dysfunction. The causal relationship between the cell-cycle balance and the expression of SD components is uncertain. It is generally observed that the expression of differentiated functional molecules is lower in cells whose negative regulation of cell-cycle balance is altered. Several investigations have suggested that cell-cycle regulatory proteins may regulate the expression of differentiated functional molecules (22,23). Conversely, some reports have shown that the expression of the intercellular junctional complex plays a role in regulating the cell cycle (32,33). It is conceivable that the cell-cycle balance and the expression of molecules that appear in the differentiated phenotype of the cells must reciprocally regulate each other. However, it should be noted that the expression of cyclin A, the positive regulator of the cell cycle, was clearly heightened already on day 1 after PAN injection (Figure 5), when the lowered expression of SD components was not yet remarkable (Figure 3). This suggests that the altered cell-cycle balance gives rise to a lowered expression of SD components in PAN nephropathy. Heightened expression of cyclin A was detected in the early phase (day 1) in ANA nephropathy as well. Although the proteinuria in ANA nephropathy is considered to result directly from the SD dysfunction caused by antibody binding, this finding suggests that the altered cell-cycle balance of the podocyte contributes to the development of proteinuria in ANA nephropathy as well.

Then, we investigated whether IP-10 regulates the cell-cycle balance. The effects of the rIP-10 treatment and the anti–IP-10 function-blocking antibody treatment on the expression of the cell-cycle regulatory proteins in the cultured podocytes were analyzed. Western blot analysis showed that rIP-10 treatment heightened the expression of $p27^{Kip1}$ and $p57^{Kip2}$ in the cultured podocytes, whereas it lowered the expression of cyclin E, cyclin A, and pRb. The $p27^{Kip1}$ that is enhanced by IP-10 may downregulate the expression of cyclin E, cyclin A, and pRb (Figure 6A). We also showed that rIP-10 treatment inhibited the proliferation of permissive conditioned podocyte (Figure 6B). It is not clear whether this effect of IP-10 is through CXCR3 receptor, because the expression of CXCR3 was rarely detected in permissive conditioned podocyte. Whatever their precise mechanism is, these findings clearly indicate that IP-10 contributes to the regulation of the expression of cell-cycle regulatory proteins and also to the inhibition of the proliferation of podocyte. These effects of rIP-10 were neutralized or reversed by co-incubation with anti–IP-10 function-blocking antibody. Anti–IP-10 mAb treatment without rIP-10 pretreatment clearly heightened the expression of cyclins E and A and lowered the expression of $p27^{Kip1}$ and $p57^{Kip2}$, which means that anti–IP-10 mAb blocked endogenous IP-10 in the cultured podocytes. Recently, siRNA has become a specific and useful technique to turn off the expression of target genes (34). To reduce the expression of cyclin A and $p27^{Kip1}$, we used siRNA targeting the two molecules. The expression of IP-10 and SD components was heightened by the treatment of siRNA of cyclin A. The treatment with siRNA $p27^{Kip1}$ lowered the expression of IP-10 and SD components (Figure 7). The finding clearly showed the link between cell-cycle protein and IP-10 and SD components. The effects of IP-10 on the regulation of the cell cycle were confirmed by *in vivo* studies on rats treated with anti–IP-10 mAb. The rats that received injections of anti–IP-10 mAb showed a clearer expression of cyclins E and A than the rats that received injections of irrelevant antibodies (Figure 8). These data clearly show that, *in vivo*, IP-10 is involved in the regulation of the cell-cycle pathways. Luster *et al.* (35) stated that IP-10 inhibits endothelial cell proliferation as well as platelet factor 4 (PF4). Romagnani *et al.* (36) reported that CXCR3